

Ionic liquids and deep eutectic solvents as gas chromatographic stationary phases for separation and characterization

by

Gabriel A. Odugbesi

A thesis submitted to the graduate faculty
in partial fulfillment of the requirements for the degree of
MASTER OF SCIENCE

Major: Analytical Chemistry

Program of Study Committee:
Jared Anderson, Major Professor
Robyn Anand
Vincenzo Venditti

The student author, whose presentation of the scholarship herein was approved by the program of study committee, is solely responsible for the content of this thesis. The Graduate College will ensure this thesis is globally accessible and will not permit alterations after a degree is conferred.

Iowa State University

Ames, Iowa

2020

Copyright © Gabriel A. Odugbesi, 2020. All rights reserved.

TABLE OF CONTENTS

	Page
ACKNOWLEDGMENTS	iv
ABSTRACT.....	v
CHAPTER 1. GENERAL INTRODUCTON	1
Introduction	1
Brief introduction to ionic liquids	1
Ionic liquids as gas chromatographic stationary phases.....	1
Thermal stability of ionic liquids	3
Deep eutectic solvents	4
Deep eutectic solvents as GC stationary phases.....	5
CHAPTER 2. ULTRA-HIGH THERMAL STABILITY IONIC LIQUIDS AS GAS CHROMATOGRAPHIC STATIONARY PHASES FOR THE SELECTIVE SEPARATION OF POLYAROMATIC HYDROCARBONS AND POLYCHLORINATED BIPHENYLS	7
Abstract.....	7
Introduction	8
Materials and Method.....	11
Materials	11
Synthesis of ionic liquids	12
GC column preparation	15
Preparation of probe solute standards and chromatographic conditions.....	15
Results and Discussion	17
Evaluation of thermal stability of IL-based stationary phases using GC-FID	18
Chromatographic selectivity of IL-based stationary phases for PAHs	20
Separation of PCB mixture on IL-based stationary phases	21
Solvation parameter model.....	23
Conclusion	24
Acknowledgments	25
References	26
Figures	30
Tables.....	33
Supplemental	36
CHAPTER 3. CHARACTERIZING THE SOLVATION INTERACTIONS OF DEEP EUTECTIC SOLVENTS BY ABRAHAM SOLVATION PARAMETER MODEL	47
Abstract.....	47
Introduction	47

Materials and Methods	52
Materials	52
Synthesis of DES	53
Coating of DES as a stationary phase	54
Results and Discussion	55
Effect of the hydrogen bond acceptor	57
Effect of hydrogen bond donor	58
Desulfurization of fuels with DES	59
Extraction of natural products Cynaropicrin	60
Conclusion	61
References	62
Figures	67
Tables	69
Supplemental	76
CHAPTER 4. GENERAL CONCLUSION	78

ACKNOWLEDGMENTS

I would like to thank my advisor, Dr. Jared Anderson for his supervision and guidance during my time here at Iowa State University. I am grateful for the knowledge I've acquired over the three years in the Anderson group. I'd also like to thank my committee members: Dr. Venditti and Dr. Anand for their support, feedback and time. I'd like to thank current and former group members: He Nan, Kevin Clark, Stephen Pierson, Marcelino Varona, Chenghui Zhu, Han Chen, Qamar Farooq, Nabeel Abbasi, Philip Eor, and Miranda Emaus. Thanks to all the visiting professors and visiting scholars that had the opportunity to work in our group: Dr. Maria José Trujillo-Rodríguez, Dr. Dongmei Lu, Dr. X-Tian Peng, Dr. Xiong Ding, and Dr. Deepak Chand. I'd also like to thank my parents, Risikat and Ademola Odugbesi as well as my siblings, Samuel and Adeola for their continuous support of my education. I am grateful for the positive feedback and moral support through this journey. Finally, I'd like to thank my friends, colleagues and the staff/faculty in the chemistry department at Iowa State University.

ABSTRACT

Recent developments have been made to improve the separation of complex molecules. The following chapters describe the optimization and characterization of two unique stationary phases: ionic liquids (ILs) and deep eutectic solvents (DESs). The versatility of ILs have expanded over the years and one of their most interesting applications are their use as gas chromatographic stationary phases. As shown in literature, they can either act as a nonpolar or polar phase depending on the analytes of interest. By manipulating the structure of the ILs, the molecular interactions exhibited between the stationary phase and probes can be tailored for favorable interactions. Imidazolium and phosphonium ILs are commonly used as cations with a variety of different counter anions. One of the major drawbacks of ILs is their low thermal stabilities compared to many other commercial phases. The first study addresses this by incorporating phenyl substituents within the cation to reduce the probability of decomposition pathways. High boiling point analytes such as polycyclic aromatic hydrocarbons (PAHs) and polycyclic biphenyls (PCBs) were separated due to their capability of undergoing π - π interactions with the stationary phase. The second study is also relating to molecular interactions but instead of an IL-based stationary phase, DESs were the materials of interest. Using multiple combinations of hydrogen bond acceptors and donors to form the DESs, in depth molecular insight was gained using inverse gas chromatography (GC). The Abraham solvation parameter model was used to characterize the deep eutectic based stationary phases. As stationary phases, both materials displayed unique interactions where the ILs showed enhanced π - π interactions while the DESs displayed increased hydrogen bond basicity compared to traditional ILs.

CHAPTER 1. GENERAL INTRODUCTON

Introduction

Brief introduction to ionic liquids

ILs are classified as nonmolecular ionic solvents with low vapor pressures and melting points below 100 °C [1]. These molten salts are generally composed of an organic cation and inorganic or organic anion (See figure 1). Over the last twenty years, the use of ILs has expanded in various areas of chemistry, including sample preparation [2], solvents for organic synthesis [3], and gas chromatographic stationary phases [4,5]. The selectivity for a given application can be improved by making structural modifications to the ILs for the exploration of new interactions via synthesis.

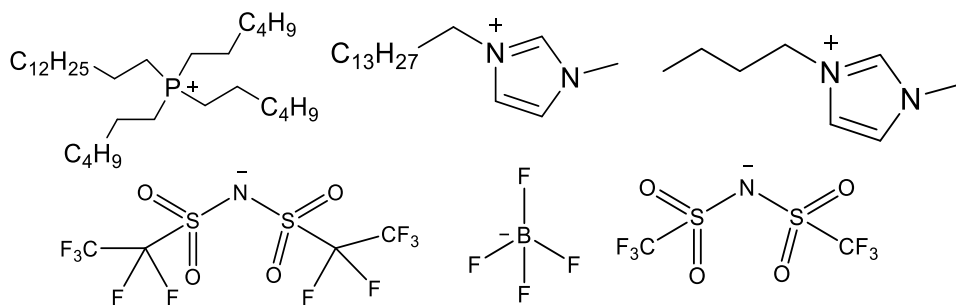


Figure 1. Various structures of traditional IL anions and cations

Ionic liquids as gas chromatographic stationary phases

Gas chromatography (GC) is a technique used to separate small molecules in their gaseous state using an immobilized stationary phase. In gas-liquid chromatography (GLC), molecules are injected inside a column, and they experience partitioning between a liquid stationary phase and a gaseous mobile phase (e.g., helium). Most nonpolar commercial GC stationary phases include a polydimethylpolysiloxane (PDMS) backbone, while polar phases consist of polyethylene glycol (PEG). The unique selectivity and tunability of ILs make them advantageous, whereas they can act as a polar or nonpolar phase.

To utilize an IL as a stationary phase for GC analysis, the phase must first be coated within the capillary. The static coating method has been employed to efficiently coat a thin layer of the stationary phase within the wall of the capillary. This technique requires the stationary of choice to be soluble in a solution that would be later removed by evaporation. It is shown in equation 1, the film thickness (d_f) of the phase can be approximated using the concentration of the solution and inner diameter of the capillary.

$$d_f = \frac{d \times c}{400}$$

Equation 1. Calculation of the film thickness using the static coating method technique.

As shown in figure 2, the thin layer of the stationary phase (280 nm) is immobilized within the fused silica capillary, where the mobile phase passes over. Once the column is coated, the column is conditioned at temperatures below the maximum allowable operating temperature (MAOT) to ensure the removal of impurities and prevent column degradation. The analytes are approximately 0.1 nm in length, are then passed through the column via partitioning between the stationary phase and mobile phase [6]. As GC stationary phases, ILs exhibit selectivity based on the chemical structure and combination of anions and cations. It was reported that ILs containing halogen anions (e.g., $[\text{Cl}^-]$) displayed much stronger retention for probe molecules containing acidic protons, while anions such as $[\text{PF}_6^-]$ resulted in much weaker retention times [7]. The addition of $[\text{Cl}^-]$ within the chemical structure gives rise to strong hydrogen bonding interaction and hence longer retention times.

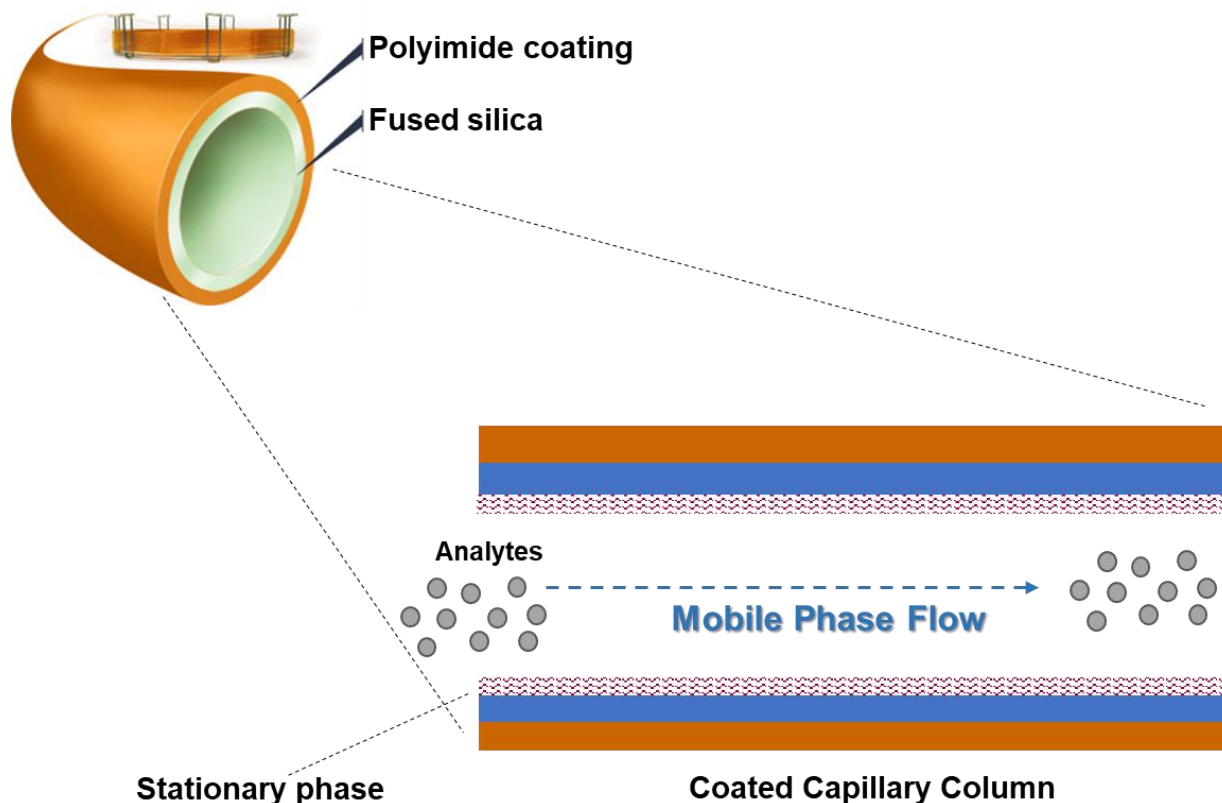


Figure 2. General scheme of WCOT column using a fused silica capillary

Thermal stability of ionic liquids

While ILs have proven to be beneficial in GLC, one of their major drawbacks has been their limited thermal stability. Compared to commercially available stationary phases, ILs are at a slight disadvantage when it comes to applications requiring high oven temperatures. Compared to monocationic ILs, dicationic ILs offers slightly higher thermal stability due to their increased charge density [8]. The decomposition of traditional IL-based stationary phases is back to its cation, where studies have shown that tetralkylphosponium and n-functionalized azaheterocycles undergo Hofmann elimination as temperature rises [9,10]. To address this issue, Davis and coworkers replaced the alkyl side chain substituents with aryl groups (See figure 3 below).

The removal of a proton on the aryl groups of the cation will produce benzyne intermediates, which are known to be unstable [10,11]. While this reaction is still plausible, very

high temperatures are required as well as the presence of a superbase over the traditional $[\text{Ntf}_2]^-$ anion. As shown in figure 3, each IL possesses the same $[\text{Ntf}_2]^-$ anion with unique aryl functionality to suppress the common decomposition pathways. Given the distinct structural features, they displayed strong π - π interactions with analytes as well as high thermal stabilities ranging from 290 to 350 °C.

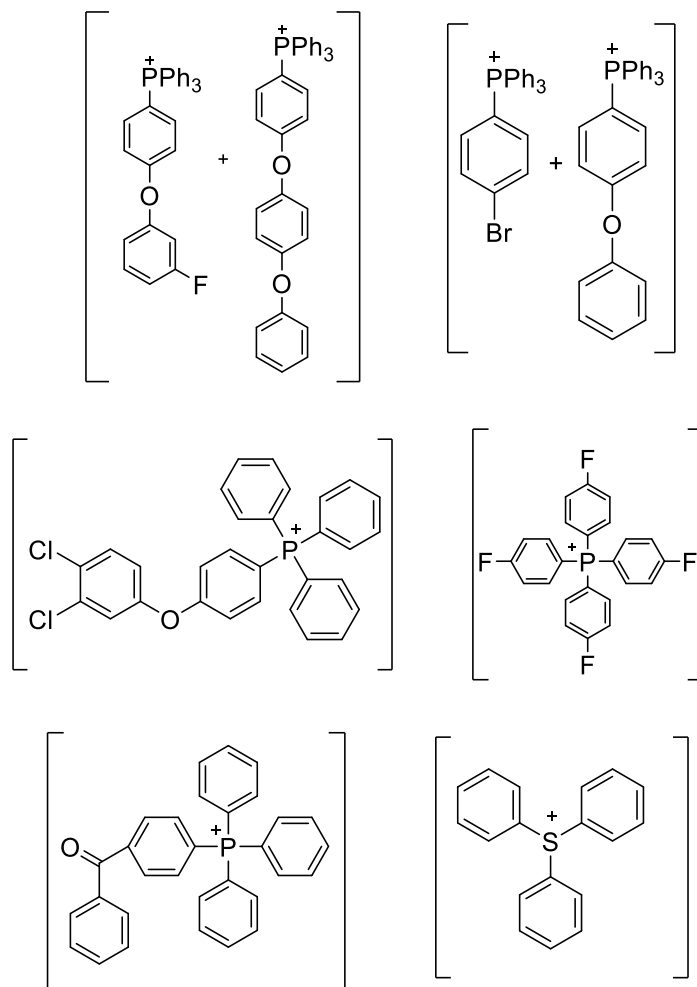


Figure 3. Structure of arylated cation proposed for high-temperature study

Deep eutectic solvents

Deep eutectic solvents (DESs) are low melting point liquids that are formed by mixing relative ratios of a hydrogen bond donor (HBD) and hydrogen bond acceptor (HBA) [12]. Common HBDs include alcohols, carboxylic acids, and amides, while HBAs generally consist of

quaternary ammonium or phosphonium salts [13]. The salt component of these solvents consists of IL-based, where a distinct anion and cation is present. Unlike ILs, DESs undergo not only electrostatic interaction but are capable of hydrogen bonding due to the presence of the halide (e.g., $[\text{Cl}^-]$) and HBD. The hydrogen bonds occurring in these solvents are responsible for the low melting points as both the HBA and HBD possess higher melting points individually. Compared to ILs, DESs have also been applied as extraction solvents [14], solvents in nanotechnology [15], and carbon dioxide capture [16].

Deep eutectic solvents as GC stationary phases

In this study, DESs were used as GC stationary phases for the first time to characterize their molecular interactions chromatographically. Like ILs, the structural features of these solvents can be tuned as well as their relative ratios for targeted applications. Synthetically, these compounds can be prepared readily at low cost with little to no toxicity due to the lack of workup required [17]. Spectroscopic methods such as the use of the Kamlet-Taft parameters and normalized polarity scales have been used to evaluate their polarities and interaction capabilities. While many of these techniques have been devised over the years, they fail to address every possible interaction as DES possessing different HBA and HBD appear to have similar polarities [18].

Inverse GC is a technique that studies the partitioning of a pure compound isothermally to gain insight on the stationary phases' ability to form interactions. A chromatographic method known as the Abraham solvation parameter model employed inverse GC and was used for the first time to characterize these DES. Unlike previous methods, the Abraham model includes a wide variety of probe molecules (over 4000) compared to the solvatochromic probes for adequate characterization of possible interactions. While using only milligram amounts of the

DES, solvation properties of the DES were studied at three temperatures to gain insight on molecular interactions [5,19]. A series of 20 ammonium and phosphonium HBAs with varying hydrogen bond donors (e.g., carboxylic acids) were among the many DES included in this study. The interaction parameters based on the effect of the pKa of acids, the molar ratio of HBA to HBD, and chain lengths were examined using this model.

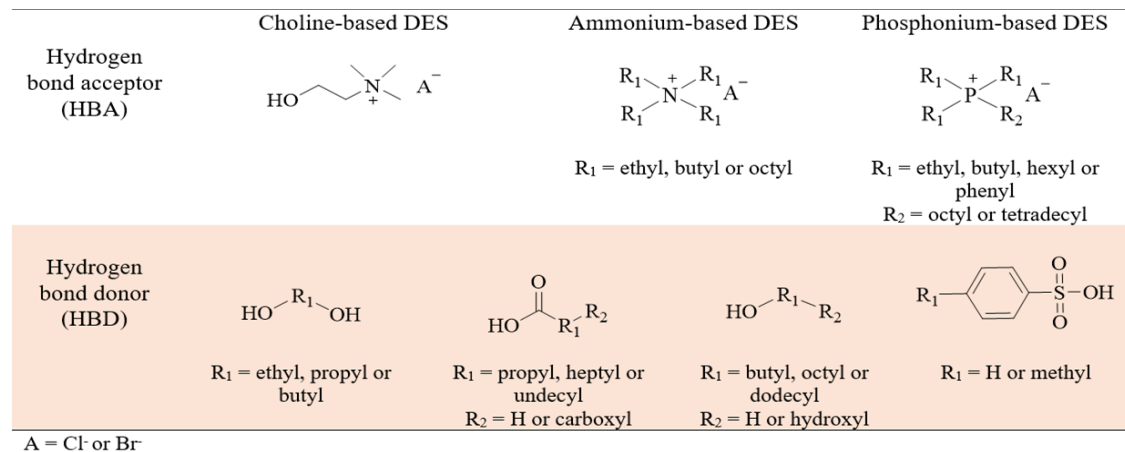


Figure 4. Structures of common DES combinations available

Inverse GC is a technique that studies the partitioning of a pure compound isothermally to gain insight on the stationary phases' ability to form interactions. A chromatographic method known as the Abraham solvation parameter model employed inverse GC and was used for the first time to characterize these DES. Unlike previous methods, the Abraham model includes a wide variety of probe molecules (over 4000) compared to the solvatochromic probes for adequate characterization of possible interactions. While using only milligram amounts of the DES, solvation properties of the DES were studied at three temperatures to gain insight on molecular interactions [5,19]. A series of 20 ammonium and phosphonium HBAs with varying hydrogen bond donors (e.g., carboxylic acids) were among the many DES included in this study. The interaction parameters based on the effect of the pKa of acids, the molar ratio of HBA to HBD, and chain lengths were examined using this model.

CHAPTER 2. ULTRA-HIGH THERMAL STABILITY IONIC LIQUIDS AS GAS CHROMATOGRAPHIC STATIONARY PHASES FOR THE SELECTIVE SEPARATION OF POLYAROMATIC HYDROCARBONS AND POLYCHLORINATED BIPHENYLS

Gabriel A. Odugbesi,^a He Nan,^a Mohammad Soltani,^b James H. Davis Jr,^b Jared L. Anderson^{a,*}

^aDepartment of Chemistry, Iowa State University, Ames, Iowa 50011, USA

^bDepartment of Chemistry, University of South Alabama, Mobile, Alabama 36688, USA

Modified from a manuscript, published in Journal Chromatography A

Abstract

Ionic liquids (ILs) are well-known in the field of separation science for their unique selectivity when used as stationary phases in gas chromatography (GC). While a significant amount of knowledge has been attained in correlating structural features of an IL to separation selectivity, developments in producing IL-based stationary phases suitable for high temperature GC studies have lagged behind. Column bleed is a result of the stationary phase undergoing volatilization /decomposition at high temperatures and is undesirable in separations coupled to GC/MS. It has been well-known that traditional classes of ILs with long alkyl side chain substituents are susceptible to Hofmann elimination at elevated temperatures. In this study, a new class of IL stationary phases containing perarylated cations exhibiting improved thermal stability are introduced. These ILs were used to prepare wall-coated open tubular columns with high column efficiency and produced very low bleed at temperatures up to 350 °C. Their unique chemical structures provide stronger π - π interactions compared to many commercially-available stationary phases. To exploit the unique interactions provided by these stationary phases, the separation of two classes of environmentally hazardous aromatic compounds, namely, polycyclic aromatic hydrocarbons (PAHs) and polychlorinated biphenyls (PCBs), was examined. Both classes of compounds contain structural isomers with high boiling points that are often

challenging to separate. The perarylated sulfonium and phosphonium IL-based stationary phases exhibited excellent thermal stability as well as unique selectivity toward isomers of PAHs as well as toxic PCB analyte pairs.

Keywords: gas chromatography; ionic liquids; polycyclic aromatic hydrocarbons; polychlorinated biphenyls; solvation parameter model

Introduction

Ionic liquids (ILs), classified as non-molecular ionic solvents, are composed of an organic cation and an inorganic/organic anion [1]. ILs possess a number of unique features such as tunable physiochemical properties, low melting points, high thermal stability, and negligible vapor pressure at ambient temperatures [2]. In the field of analytical chemistry, ILs have been widely studied in chromatographic separations, electrochemical sensing, and sample preparation [2–5]. When used as stationary phases in gas chromatography (GC), ILs exhibit unique chromatographic selectivity toward different classes of analytes that is often based on the chemical structure and combination of cations and anions [4,6].

Compared to a number of commercial stationary phases (e.g., HP-5 and SPB-50), IL-based stationary phases generally offer lower thermal stabilities, placing them at a disadvantage when high separation temperatures are required. Increased column bleed originating from thermal decomposition/volatilization of the stationary phase can lower the signal-to-noise ratio for analytes and lead to poor sensitivity [7]. To improve the chromatographic performance of the stationary phase at high temperatures, commercially-available columns are often highly crosslinked using silarylene-siloxane copolymers to prevent ion source contamination when used in mass spectrometry (MS) [8]. GC/MS compatible stationary phases provide very low bleed profiles at elevated temperatures making them highly attractive in the separation of compounds with high boiling points. To exploit the unique separation power of IL-based stationary phases in

GC/MS methods, their thermal stabilities must be improved. Recent studies have shown that imidazolium/phosphonium-based ILs with aryl substituents exhibit excellent thermal stability [9]. In addition, these ILs have the potential to provide strong π - π interactions toward analytes containing aromatic functionality. These ILs represent a class of compounds that have great potential in the separation of high molecular weight and thermally-stable organic compounds when used as stationary phases.

Polycyclic aromatic hydrocarbons (PAHs) and polychlorinated biphenyls (PCBs) are among the more challenging high molecular weight analytes to separate by GC. PAHs are composed of multiple fused aromatic rings and the numerous isomers of these compounds are often targeted in the analysis of environmental samples [10]. They are generated primarily from the incomplete combustion of fossil fuels [11]. PCBs are a group of persistent environmental contaminants that can be found in the fatty tissues of animals and humans due to their hydrophobicity and resistance toward metabolism. Before any health and environmental restrictions were put into place, PCBs were used as fire retardants and insulating fluids in electrical capacitors leading to their widespread existence in the environment [12]. The analysis of PAHs and PCBs dates back to the early 1970s using GC with porous-layer open tubular (PLOT) and wall-coated open tubular (WCOT) columns [13,14]. Although the separation of a wide range of PAHs have been studied, certain isomers with high boiling points, such as benzo[j]fluoranthene and benzo[b]fluoranthene, are often poorly separated [15]. In the case of PCBs, the analytical challenge results from the large amount of possible congeners, where the separation of all isomers is difficult to achieve on one single column [16–18]. Due to the similar chemical and physical properties of all 209 possible congeners, co-elution is a significant challenge.

To adequately separate PAHs and PCBs, stationary phases based on polydimethylsiloxane (PDMS) containing varying amounts of dimethyl and diphenyl modification have been widely studied [19]. Shape selective stationary phases such as the C60 fullerene phase have been shown to exhibit better selectivity for planar PCBs. However, the high column bleed of this stationary phase at elevated oven temperatures precluded the separation of high boiling point congeners [20]. To resolve the structural isomers for both classes of analytes, IL-based stationary phases have been explored due to their unique chromatographic selectivity [21]. Monocationic IL-based stationary phases, including 1-benzyl-3-methylimidazolium triflate and 1-(4-methoxyphenyl)imidazolium triflate, were shown to exhibit thermal stabilities up to 260 °C [22]. Dicationic ILs were subsequently developed and their thermal stabilities were found to be higher than their monocationic analogues [23]. Dicationic imidazolium IL-based stationary phases with varying linker chain lengths were further developed by Armstrong and co-workers [24]. Improved separation of the benzo[j]fluoranthene and benzo[b]fluoranthene structural isomers was observed compared to PDMS stationary phases. While dicationic imidazolium IL-based stationary phases show improved stability, they are still susceptible to decomposition at high temperatures.

Recently, it was reported that the instability of conventional IL cations (e.g., N-functionalized aromatic azaheterocycles, tetralkylphosphonium) resulted from a retro-Menschutken reaction or Hofmann elimination at elevated temperatures [25,26]. To improve the thermal stability of IL cations, sulfonium- and phosphonium-based cations with aryl moieties were reported by Davis and coworkers in an effort to suppress the thermal decomposition of conventional ILs by avoiding alkyl side chain substituents [27,28]. The removal of a hydrogen atom on the aryl substituents was found to produce unstable benzyne intermediates, hence

preventing the common decomposition pathway. Therefore, sulfonium- and phosphonium-based ILs with aryl moieties hold promise as high thermal stability stationary phases that offer unique chromatographic selectivity for aromatic compounds.

In this study, six sulfonium- and phosphonium-based ILs with low melting points were designed and prepared as stationary phases for the separation of PAHs and PCBs. These IL-based stationary phases provided improved resolution of structural isomers with high boiling points from both classes of analytes compared to commercial PDMS- and IL-based stationary phases such as HP-5ms, SPB-50, and SLB-IL111. The Abraham solvation parameter model was used to study the unique solvation characteristics offered by these stationary phases. This new class of stationary phases exhibit strong π - π interactions with analytes while providing thermal stabilities ranging from 290-350 °C.

Materials and Method

Materials

Naphthalene (99%), acenaphthene (99%), fluorene (98%), phenanthrene (98%), anthracene (97%), fluoranthene (98%), pyrene (98%), benzo(a)fluoranthene (99.5%), benzo(b)fluoranthene (99.9%), and benzo(k)fluoranthene (99.5%) were purchased from MilliporeSigma (Bellefonte, PA, USA). Butyraldehyde (99%), 1-chlorobutane (99%), ethyl acetate (99.5%), methyl caproate (99%), and 2-nitrophenol (99%) were purchased from Acros Organics (Morris Plains, NJ, USA). Bromoethane (98%) was purchased from Alpha Aesar (Ward Hill, MA, USA). Ethyl benzene was purchased from Eastman Kodak Company (Rochester, NJ, USA). Acetic acid (99.9%), N,N-dimethylformamide (99.9%), and toluene (99.8%) were purchased from Fisher Scientific (Pittsburgh, PA, USA). 2-chloroaniline (98%), p-cresol (99%), o-xylene (97%), p-xylene (99.5%), and 1-bromohexane (98%) were purchased from Fluka (Steinheim, Germany). Benzaldehyde (99%), 5-bromoacenaphthene (90%), 2-

nitronaphthalene (85%), 1-chlorohexane (99%), 1-chlorooctane (99%), cyclohexanol (99%), cyclohexanone (99.8%), 1-iodobutane (99%), 1-nitropropane (98%), octylaldehyde (99%), 1-pentanol (99%), 2-pentanone (99%), propionitrile (99%), 1-decanol (99%), acetophenone (99%), aniline (99.5%), benzonitrile (99%), benzyl alcohol (99%), 1-bromooctane (99%), 1-butanol (99.8%), 1,2-dichlorobenzene (99%), dichloromethane (99.8%), 1,4-dioxane (99.5%), 1-octanol (99%), phenol (99%), pyridine (99%), pyrrole (98%), m-xylene (99.5%), 2-propanol (99.9%), and propionic acid (99%) were purchased from MilliporeSigma. The reagents 4-fluoriodobenzene, Tris(4-fluorophenyl)phosphine, Pd(OAc)₂, potassium bis[(trifluoromethyl)sulfonyl]imide, 1,2-dichloro-4-(4-iodophenoxy)benzene, 1,4-diiodobenzene, potassium carbonate, copper(II) oxide, and 3,4-dichloro phenol were purchased from Sigma-Aldrich. A PCB calibration check solution containing 21 different congeners at a concentration of 100 µg/mL in acetone was purchased from Accustandard (New Haven, CT, USA). The chemical names and molecular structures for the PAHs and PCBs are listed in Tables S1 and S2 (see supporting information). The columns SLB-5ms (30 m × 250 µm × 0.25 µm), SPB-50 (30 m × 250 µm × 0.25 µm), and SLB-ILPAH (20 m × 180 µm × 0.05 µm) were purchased from MilliporeSigma (Bellefonte, PA, USA). The HP-5ms (30 m × 250 µm × 0.25 µm) and HP-5ms UI (30 m × 250 µm × 0.25 µm) columns were obtained from Agilent Technologies (Santa Clara, CA, USA).

Synthesis of ionic liquids

The chemical names and molecular structures of the ILs examined in this study are shown in Table 1. ILs 1-2 were prepared using previously reported methods [27-29]. NMR spectra were recorded on a 500 MHz JEOL spectrometer using CDCl₃ as a solvent at room temperature. All chemical shifts for ¹H and ¹³C NMR were reported downfield using tetramethylsilane (TMS, at δ ¼ 0.00 ppm).

Synthesis of IL 3: In a 50 mL heavy wall pressure vessel with an internal thread containing a stir bar, 4-fluoroiodobenzene (1.0 equiv), tris(4-fluorophenyl)phosphine (1.0 equiv), Pd(OAc)₂ (1.5 mol %) and xylene (15 mL) were added under nitrogen atmosphere and reaction mixture stirred at 140 °C for 2 hours. The reaction mixture was then cooled down to room temperature and filtered to yield pure tetra(4-fluorophenyl) phosphonium iodide as a pale solid. The [NTf₂-] salt was achieved by anion exchange of [K⁺] [NTf₂-] (1.0 equiv) and the phosphonium salt (1.0 equiv) in water for 15 min at room temperature. The reaction mixture was then extracted three times with dichloromethane and brine solution. The combined organic extracts were dried over anhydrous Na₂SO₄, solvents were removed under reduced pressure, and pure tetra(4-fluorophenyl) phosphonium [NTf₂-] was achieved as a white solid. Pure crystals of the product were achieved by crystallization in hot ethanol. ¹H NMR (CDCl₃, 500 MHz): δH 7.65-7.61 (m, 8H), 7.42-7.39 (m, 8H); ¹³C NMR (CDCl₃, 125 MHz): δC 168.0 (d), 165.9 (d), 137.1 (t), 123.3, 120.8, 118.5 (m), 115.7, 113.2, 112.5; ³¹P NMR (CDCl₃, 202 MHz): δp 22.50 ppm; ¹⁹F NMR (CDCl₃, 470 MHz): -78.96, -98.77 ppm. T_m = 137 °C (+/- 1.0 °C).

Synthesis of IL 4: First, 1,2-dichloro-4-(4-iodophenoxy)benzene was synthesized by mixing 1,4-diiodobenzene (1.0 equiv), potassium carbonate (2.5 equiv), copper(II) oxide (2.5 equiv), and 3,4-dichlorophenol in DMF as a solvent at 120 °C for overnight. After completion of the reaction, the pure compound was achieved by column chromatography. Then, 4-(3,4-dichlorophenoxy)phenyltriphenylphosphonium [NTf₂-] was prepared following the general procedure. ¹H NMR (CDCl₃, 500 MHz): δH 7.87-7.84 (m, 3H), 7.75-7.71 (m, 6H), 7.61-7.57 (m, 6H), 7.57-7.52 (m, 2H), 7.48-7.47 (m, 1H), 7.24-7.22 (m, 3H), 7.05-7.03 (m, 1H); ¹³C NMR (CDCl₃, 125 MHz): δC 163.1, 152.7, 136.7 (d), 135.5 (d), 133.6, 131.7, 13.6 (d), 129.3, 122.7,

121.0, 120.4, 118.9, 118.8, 118.4, 117.9, 117.2, 110.5, 109.8; ^{31}P NMR (CDCl_3 , 202 MHz): δ_{p} 23.28 ppm; ^{19}F NMR (CDCl_3 , 470 MHz): -78.62 ppm. $T_{\text{g}} = 3.0 \text{ }^{\circ}\text{C}$ ($\pm 0.05 \text{ }^{\circ}\text{C}$).

Synthesis of IL 5: 4-bromophenyltriphenylphosphonium [NTf_2^-] and 4-phenoxyphenyltriphenylphosphonium [NTf_2^-] were first prepared following the general procedure. Then, an equimolar ratio of these two compounds was combined and melted to produce the desired IL. ^1H NMR (CDCl_3 , 500 MHz): δ_{H} 7.94-7.90 (m, 2H), 7.86-7.84 (m, 8H), 7.76-7.71 (m, 12H), 7.64-7.55 (m, 16H), 7.48-7.41 (m, 5H); ^{13}C NMR (CDCl_3 , 125 MHz): δ_{C} 148.08, 138.08, 135.82-135.56 (m) 134.70 (d), 134.24 (d), 133.95 (d), 130.70 (d), 129.22, 128.95 (d), 127.37, 123.64, 121.08, 118.52, 117.88, 117.25 (d), 116.97, 116.53, 116.25, 115.96, 115.73, 115.01. ^{31}P NMR (CDCl_3 , 202 MHz): δ_{p} 23.98, 23.68 ppm; ^{19}F NMR (CDCl_3 , 470 MHz): -78.60 ppm. $T_{\text{g}} = 2.6 \text{ }^{\circ}\text{C}$ ($\pm 0.14 \text{ }^{\circ}\text{C}$).

Synthesis of IL 6: The ILs 4-[4-(4-phenoxyphenoxy)phenoxy]phenyltriphenylphosphonium [NTf_2^-] and 4-[4-(3-fluorophenoxy)phenoxy]phenyltriphenylphosphonium [NTf_2^-] was prepared following the general procedure. Then, an equimolar ratio of these two compounds was combined and melted to result the desired IL. ^1H NMR (CDCl_3 , 500 MHz): δ_{H} 7.86-7.84 (m, 6H), 7.74-7.73 (m, 12H), 7.63-7.57 (m, 12H), 7.54-7.49 (m, 4H), 7.40-7.38 (m, 1H), 7.33-7.30 (m, 2H), 7.23-7.21 (m, 4H), 7.10-7.08 (m, 3H), 7.03-7.02 (m, 2H), 6.99-6.98 (m, 2H), 6.95-6.93 (m, 2H), 6.85-6.83 (m, 1H); ^{13}C NMR (CDCl_3 , 125 MHz): δ_{C} 164.5 164.4, 163.5, 162.4, 156.8, 154.8, 136.5 (t), 135.5, 134.2 (d), 130.6 (m), 129.8, 123.5, 122.2, 121.1, 120.3, 118.9-118.0 (m), 117.5, 117.3, 116.4, 112.8, 112.6, 110.1, 109.1, 108.6, 108.4, 108.3 ppm; ^{31}P NMR (CDCl_3 , 202 MHz): δ_{p} 23.28, 23.24 ppm; ^{19}F NMR (CDCl_3 , 470 MHz): -78.60, -109.38 ppm. $T_{\text{g}} = 10.0 \text{ }^{\circ}\text{C}$ ($\pm 0.03 \text{ }^{\circ}\text{C}$).

GC column preparation

Using the static coating method, thirty-meter untreated fused silica capillaries were coated with the ILs examined in this study. The coating solution was prepared by dissolving the ILs in dichloromethane at a concentration of 0.32% (w/v) to yield an approximate film thickness of 0.20 μm . The coated columns were conditioned at 200 $^{\circ}\text{C}$ for 12 h under a constant flow of helium. The column efficiency was determined using naphthalene at 110 $^{\circ}\text{C}$. The list of columns examined in this study and their characteristics is shown in Table 2. All columns possessed efficiencies higher than 3700 plates/meter.

Preparation of probe solute standards and chromatographic conditions

The PAH mixture was prepared by dissolving the analytes in hexane at a concentration of 0.5 mg/mL. The PAH standards were prepared in hexane at a concentration of 0.1 mg/mL. The PAH separations were performed on an Agilent 7890B gas chromatograph coupled to a flame ionization detector (GC-FID). Helium was used as the carrier gas at a flow rate of 1 mL/min. The injector and detector temperatures were held at 250 $^{\circ}\text{C}$ using a split ratio of 20:1 and an injection volume of 1 μL . The detector employed hydrogen as the makeup gas at a flow rate of 30 mL/min, while the air flow was held at 400 mL/min. The temperature program for the analysis of PAHs was optimized for each column to achieve the best separation.

The PCB mixture was diluted from the standard solution to a concentration of 8 $\mu\text{g/mL}$. Separation of the mixture was performed on an Agilent 7890B/5977A GC/MS system. Helium was employed as the carrier gas at a flow rate of 1 mL/min and all injections were performed in split mode at a split ratio of 5:1. The temperature program for the analysis of PCB mixture was optimized for each column. For the HP-5ms UI column, the oven temperature was initially held at 125 $^{\circ}\text{C}$, then increased to 185 $^{\circ}\text{C}$ at a rate of 12 $^{\circ}\text{C/min}$ and held for 2 min. The temperature was then ramped to 220 $^{\circ}\text{C}$ at a rate of 10 $^{\circ}\text{C/min}$ with a hold time of 2 min, and finally ramped

to 250 °C at a rate of 12 °C/min. For the SLB-IL111 column, the oven temperature was initially held at 85 °C, then increased to 190 °C at a rate of 8 °C/min and held for 3 min. The temperature was then ramped to 235 °C at a rate of 8 °C/min with a hold time of 6 min, and finally ramped to 260 °C at a rate of 12 °C/min.

For IL 1, the oven temperature was initially held at 190 °C, then increased to 200 °C at a rate of 4 °C/min and held for 5 min. The temperature was ramped to 235 °C at a rate of 10 °C/min with a hold time of 5 min and finally ramped to 265 °C at a rate of 8 °C/min. For IL 2, the oven temperature was initially held at 185 °C, then increased to 200 °C at a rate of 8 °C/min with a hold time of 3 min. The temperature was then ramped to 235 °C at a rate of 6 °C/min with a hold time of 10 min, and finally ramped to 265 °C at a rate of 10 °C/min. For IL 3, the oven temperature was initially held at 130 °C, and then increased to 185 °C at a rate of 12 °C/min for and held for 1 min. The temperature was then ramped to 220 °C at a rate of 3 °C/min with a hold time of 2 min, and finally ramped to 265 °C at a rate of 12 °C/min. For IL 4, the oven temperature was initially held at 185 °C, then increased to 220 °C at a rate of 15 °C/min and held for 5 min. The temperature was ramped to 245 °C at a rate of 5 °C/min with a hold time of 5 min, and finally ramped to 265 °C at a rate of 8 °C/min. For IL 5, the oven temperature was initially held at 215 °C for 1 min, then increased to 230 °C at a rate of 25 °C/min and held for 3 min. The temperature was then ramped to 250 °C at a rate of 5 °C/min with a hold time of 6 min, and finally ramped to 285 °C at a rate of 12 °C/min. For IL 6, the oven temperature was initially held at 185 °C, then increased to 200 °C at a rate of 8 °C/min and held for 3 min. The temperature was ramped to 235 °C at a rate of 6 °C/min with a hold time of 1 min, and finally ramped to 265 °C at a rate of 10 °C/min.

For experiments involving the solvation parameter model, analytes were prepared in dichloromethane at a concentration of 1 mg/mL. All GC measurements were performed on an Agilent 7890B GC-FID instrument. Helium was used as the carrier gas at a flow rate of 1 mL/min. The injector and detector temperatures were held at 250 °C. A split ratio of 100:1 was used with an injection volume of 1 µL. The detector employed hydrogen as the makeup gas at a flow rate of 30 mL/min, while the air flow was held at 400 mL/min. A list of the 46 probe molecules along with their solute descriptors is provided in Table S3. All 46 probes were injected individually at 50, 80, and 110 °C. Lower boiling point analytes exhibited lower retention times at higher oven temperatures, while the other analytes displayed stronger retention on the stationary phase. Therefore, not all analytes listed were subjected to the regression analysis at the three temperatures studied. Multiple linear regression analysis and statistical calculations were performed using the software Analyze-it (Leeds, UK).

Results and Discussion

Highly polar and thermally-stable GC stationary phases are particularly sought after in applications involving the analysis of long chain fatty acids, polycyclic aromatic sulfur heterocycles, PAHs, and PCBs [21,30–32]. Recent studies have shown that the triarylsulfonium- and tetraarylphosphonium-based ILs exhibited excellent thermal stability in that they were heated at 300 °C for 90 days with no observable mass loss [28,29]. Perarylated ILs are highly promising to further extend the application of IL-based stationary phases for the separation of high molecular weight aromatic compounds such as PAHs and PCBs.

As shown in Table 1, six different sulfonium- and phosphonium-based ILs paired with bis[(trifluoromethyl)sulfonyl]imide ([NTf₂-]) anions were studied. Among them, IL 1 is a sulfonium-based IL containing three phenyl substituents. ILs 2-6 are phosphonium-based ILs with different aryl moieties. ILs 3 and 4 contain halide modified aryl substituents, while ILs 5

and 6 are mixtures of phosphonium-based ILs. All ILs were prepared as stationary phases in GC columns for the evaluation of their thermal stability as well as chromatographic selectivity.

Evaluation of thermal stability of IL-based stationary phases using GC-FID

The thermal stability of ILs is often evaluated by thermogravimetric analysis (TGA). However, due to the high heating ramps that are often employed (e.g., 10-20 °C/min), it has been shown that this only measures the short-term stability of the IL [25]. Studies have shown that the maximum allowable operating temperature (MAOT) of IL-based stationary phases is approximately 100 °C lower than what TGA experiments indicate [26]. Recently, the decomposition of GC stationary phases has been evaluated by exploiting the high sensitivity of flame ionization detection (FID). The FID approach is highly sensitive and can detect trace volatilization and/or decomposition products that may arise from the stationary phase during heating [24]. This method was used to determine the MAOT of stationary phases by evaluating the resolving power of the stationary phase after being thermally stressed at different temperatures [33].

In this study, each IL-based stationary phase was subjected to a series of heating experiments. Initially, five-meter segments of each column were conditioned to 100 °C, 150 °C, 200 °C, and 250 °C. After each conditioning step, the chromatographic performance of the stationary phase was evaluated by measuring the column efficiency based on the retention time and peak width of naphthalene at 100 °C, while 110 °C was used for IL 3 due to its unique retention behavior. To precisely determine the MAOT of each stationary phase, the columns were subsequently conditioned to 270 °C, 290 °C, 310 °C, 330 °C, and finally 350 °C. The same procedure was repeated to measure the column efficiency after each heating step (see Tables S4-S9).

As shown in Tables 2 and S4, when IL 1 was conditioned from 310 to 330 °C, a significant loss in column efficiency was observed indicating that the MAOT of the stationary phase is approximately 300 °C. IL 2 showed an improved thermal stability with a MAOT of approximately 310 °C, due to a drop in column efficiency being observed when the column was conditioned from 330 to 350 °C.

The MAOT of ILs 4 and 5 was found to be approximately 350 °C, which are the highest among the ILs examined in this study. IL 5 is comprised of a mixture of (4-bromophenyl)triphenylphosphonium and (4-phenoxyphenyl)triphenylphosphonium ILs, while IL 4 is a phosphonium-based IL with a dichlorophenoxy substituent. When both columns were conditioned from 330 to 350 °C, the column efficiency was maintained above 2200 plates/meter indicating the very stable nature of these stationary phases. Compared to IL 5 with a MAOT of 350 °C, IL 6 possesses a MAOT of 290 °C (see Table S9) and is also a mixture composed of two different phosphonium-based ILs. Among the ILs examined in this study, IL 3 exhibited a particularly unique behavior. Generally, after the columns were conditioned at high oven temperatures, the retention time of the naphthalene probe molecule decreased. However, the retention time of naphthalene on the IL 3 column steadily increased. After heating at 350 °C, the retention time of naphthalene increased from 2.5 to 6.9 min with the peak width increasing from 0.08 to 1.64 min, resulting in extremely low column efficiency (see Table S6 in supporting information). This retention behavior was observed previously by Betts, where the retention times of analytes on liquid crystal-based stationary phases increased as the columns were heated to temperatures beyond their melting points [34]. Compared to IL 3, all other ILs exhibited excellent durability as well as high thermal stability.

Chromatographic selectivity of IL-based stationary phases for PAHs

The most widely used analytical methods for the determination of PAHs are GC/MS and high-performance liquid chromatography (HPLC) with fluorescence detection [35,36]. In comparison, GC/MS generally provides high sensitivity and better quantification results [32]. However, due to the presence of numerous isomers with high boiling points, the number of PAHs which can be analyzed by GC is limited by the thermal stability and selectivity of the stationary phase [37]. PDMS-based stationary phases such as HP-5ms, SLB-5ms and Rtx-5ms (bonded and highly crosslinked (5%-phenyl)-methylpolysiloxane) are most commonly used for PAH separation.

To evaluate the separation performance the stationary phases examined in this study, 12 PAHs (see Table S1) were selected and separated on the IL-based stationary phases and three commercial stationary phases, including HP-5ms, SLB-5ms, and SLB-ILPAH. As shown in Figure 1A, the 12 PAHs were separated on the HP-5ms stationary phase under optimized conditions. The SLB-5ms column, which is analogous to the HP-5ms column, provided comparable separation performance, as shown in Figures 1A and 2A. The resolution of benzo(b)fluoranthene and benzo(k)fluoranthene was found to be 1.48 on the SLB-5ms column under optimized separation conditions and 1.46 on the HP-5ms stationary phase. The total separation time for the HP-5ms stationary phase was approximately 35 minutes, while the SLB-5ms phase required approximately 25 minutes.

The SPB-50 stationary phase is a relatively polar PDMS-based stationary phase with approximately 50% phenyl content which acts to increase its selectivity. As shown in Figure 2B, all analytes were baseline separated except for phenanthrene and anthracene ($R_s = 1.07$). Compared to the HP-5ms and SLB-5ms stationary phases, benzo(b)fluoranthene and benzo(k)fluoranthene were baseline separated on the SPB-50 stationary phase ($R_s = 1.52$). It is

important to note that the separation took approximately 55 minutes, which is longer than the other stationary phases. A commercial IL-based column (SLB-ILPAH) possessing a similar chemical structure to SLB-IL59 (1,12-di(triethylphosphonium)dodecane bis[(trifluoromethyl)sulfonyl]imide) with the only difference being the lower film thickness ($df = 0.05 \mu\text{m}$) was subsequently examined [7,38]. Under optimized separation conditions, all 12 PAHs were well separated within 30 minutes, as shown in Figure 1B.

The six IL-based stationary phases evaluated in this study were used for the separation of PAHs under optimized conditions. Among ILs 1-6, IL 1 displayed the lowest selectivity for phenanthrene/anthracene and benzo(b)fluoranthene/benzo(k)fluoranthene, as shown in Figures S1-S4. Figures 1C and 2C show that the separation of PAHs on ILs 4 and 5, respectively, were comparable to HP-5ms, SLB-5ms, SPB-50, and SLB-ILPAH. It is important to highlight that the IL-stationary phases are non-bonded and non-crosslinked phases and are still capable of operating at high oven temperatures (e.g., $350 \text{ }^\circ\text{C}$ for ILs 4 and 5), while maintaining high column efficiency. In addition, improved selectivity for heavier PAHs such as benzo(b)fluoranthene and benzo(k)fluoranthene was demonstrated compared to the PDMS-based stationary phases. Notably, the separation time using ILs 4 and 5 was under 30 minutes. This result highlights that IL-based stationary phases comprised of multiple aryl substituents provide unique selectivity and improved separation for heavier PAHs.

Separation of PCB mixture on IL-based stationary phases

While a total of 209 congeners exist, some PCBs are in fact more harmful than others [39]. For example, toxic PCBs such as PCBs 28, 52, 101, 138, 153, and 180 have been found to be more persistent in environmental samples than their corresponding isomers, while PCBs 77, 81, 126, 170, and 180 are relatively less toxic but are highly bioaccumulative [40]. In this study, a mixture of 21 PCBs (see Table S2) containing PCBs 28, 52, 77, 101, 126, 138, 153, 170, and

180 were separated on all six IL-based columns. The HP-5ms UI and SLB-IL111 commercial columns were used for comparison purposes.

As shown in Figure 3A, all 21 components were separated based on their boiling points on the HP-5ms stationary phase. PCB 8, containing two chlorine substituents, possesses a boiling point of 191 °C, while PCB 209 (with ten chlorine substituents) possesses a boiling point of approximately 466 °C. The SLB-IL111 column displayed a unique elution order of PCBs compared to the HP-5ms column, as shown in Figure 3B.

The separation of PCBs on the six thermally-stable ILs are shown in Figures 3C-3H. Two analyte pairs (77/138 and 108/180) co-eluted on IL 1, as shown in Figure 1C. This result indicates insufficient resolving power toward these two PCB analyte pairs. IL 2 possesses a benzoylphenyl group and does not contain any halide substituents within its chemical structure. The analyte pairs 77/138 and 108/180 were separated with a resolution of 2.23 and 1.38, respectively, on this stationary phase (see Figure 3D and Table 3). The retention order for two analyte pairs PCB 77/138 and 180/108 was reversed on ILs 3 and 4. As shown in Table 3, the resolution of PCB 77 and 138 analyte pair was 3.06 on IL 3 compared to that of 1.41 on IL 4. In addition, improved resolution of PCB 108/180 analyte pair was observed on the IL 3 stationary phase compared to that of IL 4 (see Table 3). This may be due to the addition of the four fluorine substituents, hence increasing the electron density of the cation and leading to stronger π - π interactions [41].

As shown in Table 1, ILs 5 and 6 are mixture of two tetraphenylphosphonium-based ILs. IL 5 contains a bromine substituent on one cation and a phenoxy group on the other. IL 6 has a fluorophenoxyphenyl group on one cation and a phenoxyphenoxyphenyl group on the other IL cation. As shown in Figure 3G, PCBs 44 and 101 co-eluted on IL 5, while the resolution of

44/101 was 1.43 on IL 6. PCBs 108 and 180 were separated with a resolution of 2.88 on IL 5, while the analyte pair co-eluted on IL 6 (see Table 3). In addition, the retention order of PCBs 77 and 138 possessing four and six chlorine substituents, respectively, was reversed on ILs 3 and 6, as shown in Figures 3E and 3H. All six perarylated IL-based stationary phases exhibited improved resolution of analyte pairs PCB 126/128 and 108/153, compared to the commercial HP-5ms stationary phases (see Table 3).

Solvation parameter model

The Abraham solvation parameter model has been widely used to describe multiple solvation interactions between different probe molecules and stationary phases using an inverse GC approach [42,43].

$$\text{Log } k = c + eE + sS + aA + bB + lL \quad (1)$$

In Equation 1, k is the retention factor for each analyte on the high thermal stability IL stationary phases at 50 °C, 80 °C, and 110 °C. The solute descriptors (E , S , A , B , and L) of the 46 analytes are listed in Table S3. Each term is defined as: E , the excess molar refraction calculated from the solute's refractive index; S , the solutes dipolarity/polarizability; A , the solute hydrogen bond acidity; B , the solute hydrogen bond basicity; and L , the solute gas-hexadecane partition coefficient at 298 K. Multiple linear regression analysis was performed using the solute descriptors of the probe molecules and their retention factors to determine the solvation interactions. The c term is the intercept of the regression line. The system constants (e , s , a , b , and l) determine the strength of each individual interaction. Each term is defined as follows: e , the ability of the stationary phase to interact with analytes by non-bonding or π - π interactions; s , measures the dipolarity/polarizability of the stationary phase; a , the hydrogen bond basicity of the stationary phase; b , the hydrogen bond acidity of the stationary phase; and l , measures the dispersion forces/cavity formation of the stationary phase.

To examine the effect of aryl substituents on the solvation properties of the IL-based stationary phases, the perarylated ILs 1-6 were compared to the trihexyl(tetradecyl)phosphonium bis[(trifluoromethyl)sulfonyl]imide ([P66614+][NTf2-]) IL. It has been previously reported that the [P66614+][NTf2-] IL possesses a negative e term value indicating little to no lone pair and π -electron interaction capability of the stationary phase [44]. In comparison, ILs 1-6 with multiple aryl substituents possess modest lone pair and π -electron interaction capabilities as shown in Table 4 (e term value ranging from 0.14 to 0.25 at 80 °C), which has been found in this study to play an important role in the separation of PAHs and PCBs. Among ILs 1-6, IL 1 with the triarylsulfonium cation showed the highest capability of lone pair and π -electron interactions ($e = 0.25$ at 80 °C), while IL 2 which contains the (4-benzoylphenyl)triphenylphosphonium cation displayed the lowest lone pair and π -electron interactions ($e = 0.14$ at 80 °C). It can be observed that the phosphonium-based ILs with halide substituents (ILs 3-6) possess higher lone pair and π -electron interactions (e term value ranging from 0.16 to 0.22 at 80 °C) compared to IL 2 which does not contain any halide substituent. IL 2 possesses the highest polarity/polarizability among all ILs ($s = 1.80$ at 80 °C), while IL 3 possesses the lowest polarity/polarizability ($s = 1.62$ at 80 °C). The hydrogen bond acidity of ILs 1-6 range from 0.08 to 0.47 at 80 °C, while the [P66614+][NTf2-] IL possesses a negative b term value. As shown in Table 4, IL 4 exhibited the highest dispersion forces ($l = 0.63$ at 80 °C), whereas IL 6 exhibited the lowest value ($l = 0.53$ at 80 °C). ILs 1-6 all exhibited lower dispersion forces compared to [P66614+][FeCl4-] ($l = 0.69$ at 80 °C) and [P66614+][NTf2-] ($l = 0.75$ at 70 °C) [44,45]. This result is likely due to the lack of multiple alkyl substituents within the cations of the perarylated ILs.

Conclusion

A new class of perarylated ILs with high thermal stability were successfully applied as GC stationary phases. These triarylsulfonium and tetraarylphosphonium IL-based stationary

phases displayed unique selectivity toward PAHs and PCBs compared to a broad series of commercial stationary phases. Compared to HP-5ms, SLB-5ms, and SPB-50, ILs 4 and 5 exhibited unique selectivity and improved resolution of the benzo(b)fluoranthene and benzo(k)fluoranthene isomers possessing high boiling points. A mixture of 21 PCBs were separated with optimized conditions using the six IL-based stationary phases as well as two commercial HP-5ms UI and SLB-IL111 stationary phases. The retention order of analyte pairs such as PCBs 108/180 was reversed on the IL 3 and 5 columns, compared to the widely used HP-5ms column. The elution order of PCB 77/138 remained the same on all columns except the SLB-IL111 and IL 3 columns. In addition, improved resolution of analyte pairs PCB 126/128 and 108/153 was observed on all six perarylated IL-based stationary phases compared to the commercial HP-5ms stationary phase. The solvation characteristics of these ILs were evaluated using the Abraham solvation parameter model. These ILs displayed high lone pair and π -electron interaction capability compared to conventional phosphonium ILs containing long alkyl chain substituents in the cation (e.g., [P66614⁺][NTf2⁻]). This new class of IL-based stationary phases are non-bonded and not crosslinked but exhibit increased MAOT and unique selectivity toward PAHs and PCBs, making them promising materials for a broad range of applications.

Acknowledgments

The authors acknowledge funding from Chemical Measurement and Imaging Program at the National Science Foundation (Grant number CHE-1709372). The authors thank Len Sidisky from MilliporeSigma for assistance in preparing the IL-based columns.

References

- (1) Hallett, J. P.; Welton, T. Room-Temperature Ionic Liquids: Solvents for Synthesis and Catalysis. 2. *Chem. Rev.* **2011**, *111* (5), 3508–3576.
- (2) Trujillo-Rodríguez, M. J.; Nan, H.; Varona, M.; Emaus, M. N.; Souza, I. D.; Anderson, J. L. Advances of Ionic Liquids in Analytical Chemistry. *Anal. Chem.* **2018**, *91*, 505–531.
- (3) An, J.; Rahn, K. L.; Anderson, J. L. Headspace Single Drop Microextraction versus Dispersive Liquid-Liquid Microextraction Using Magnetic Ionic Liquid Extraction Solvents. *Talanta* **2017**, *167*, 268–278.
- (4) Poole, C. F.; Poole, S. K. Ionic Liquid Stationary Phases for Gas Chromatography. *J. Sep. Sci.* **2011**, *34*, 888–900.
- (5) Wang, X.; Hao, J. Recent Advances in Ionic Liquid-Based Electrochemical Biosensors. *Sci. Bull.* **2016**, *61* (16), 1281–1295.
- (6) Anderson, J. L.; Armstrong, D. W.; Wei, G.-T. Ionic Liquids in Analytical Chemistry. *Anal. Chem.* **2006**, *78* (9), 2892–2902.
- (7) Shashkov, M. V; Sidelnikov, V. N. Mass Spectral Evaluation of Column Bleeding for Imidazolium-Based Ionic Liquids as GC Liquid Phases. *Anal. Bioanal. Chem.* **2012**, *403* (9), 2673–2682.
- (8) Bengård, A.; Blomberg, L.; Lyman, M.; Claude, S.; Tabacchi, R. Siloxane/Silarylene Copolymers as Stationary Phases for Capillary Gas Chromatography Part I: Evaluation of Silanol Terminated Dimethyl Substituted Polymers. *J. High Resolut. Chromatogr.* **1987**, *10* (5), 302–318.
- (9) Cassity, C. G.; Mirjafari, A.; Mobarrez, N.; Strickland, K. J.; O'Brien, R. A.; Davis, J. H. Ionic Liquids of Superior Thermal Stability. *Chem. Commun.* **2013**, *49* (69), 7590–7592.
- (10) Boström, C.-E.; Gerde, P.; Hanberg, A.; Jernström, B.; Johansson, C.; Kyrklund, T.; Rannug, A.; Törnqvist, M.; Victorin, K.; Westerholm, R. Cancer Risk Assessment, Indicators, and Guidelines for Polycyclic Aromatic Hydrocarbons in the Ambient Air. *Environ. Health Perspect.* **2002**, *110* (3), 451–488.
- (11) Poster, D. L.; Schantz, M. M.; Sander, L. C.; Wise, S. A. Analysis of Polycyclic Aromatic Hydrocarbons (PAHs) in Environmental Samples: A Critical Review of Gas Chromatographic (GC) Methods. *Anal. Bioanal. Chem.* **2006**, *386*, 859–881.
- (12) Loomis, D.; Browning, S. R.; Schenck, A. P.; Gregory, E.; Savitz, D. A. Cancer Mortality among Electric Utility Workers Exposed to Polychlorinated Biphenyls. *Occup. Environ. Med.* **1997**, *54*, 720–728.

- (13) Fryčka, J. Separation of Polynuclear Aromatic Hydrocarbons by Gas-Solid Chromatography on Graphitized Carbon Black Deposited on Chromosorb W. *J. Chromatogr. A* **1972**, *65* (2), 432–434.
- (14) Krupčík, J.; Leclercq, P. A.; Šimová, A.; Suchánek, P.; Čollák, M.; Hrivňák, J. Possibilities and Limitations of Capillary Gas Chromatography and Mass Spectrometry in the Analysis of Polychlorinated Biphenyls. *J. Chromatogr. A* **1976**, *119*, 271–283.
- (15) Manzano, C.; Hoh, E.; Massey Simonich, S. L. Improved Separation of Complex Polycyclic Aromatic Hydrocarbon Mixtures Using Novel Column Combinations in GC × GC/ToF-MS. *Environ. Sci. Technol.* **2012**, *46*, 7677–7684.
- (16) Mydlová-Memersheimerová, J.; Tienpont, B.; David, F.; Krupčík, J.; Sandra, P. Gas Chromatography of 209 Polychlorinated Biphenyl Congeners on an Extremely Efficient Nonselective Capillary Column. *J. Chromatogr. A* **2009**, *1216*, 6043–6062.
- (17) Muscalu, A. M.; Górecki, T. Comprehensive Two-Dimensional Gas Chromatography in Environmental Analysis. *TrAC Trends Anal. Chem.* **2018**, *106*, 225–245.
- (18) Zapadlo, M.; Krupčík, J.; Kovalczuk, T.; Májek, P.; Špáňik, I.; Armstrong, D. W.; Sandra, P. Enhanced Comprehensive Two-Dimensional Gas Chromatographic Resolution of Polychlorinated Biphenyls on a Non-Polar Polysiloxane and an Ionic Liquid Column Series. *J. Chromatogr. A* **2011**, *1218* (5), 746–751.
- (19) Seethapathy, S.; Górecki, T. Applications of Polydimethylsiloxane in Analytical Chemistry: A Review. *Anal. Chim. Acta* **2012**, *750*, 48–62.
- (20) Cochran, J. W.; Frame, G. M. Recent Developments in the High-Resolution Gas Chromatography of Polychlorinated Biphenyls. *J. Chromatogr. A* **1999**, *843* (1–2), 323–368.
- (21) Ros, M.; Escobar-Arnanz, J.; Sanz, M. L.; Ramos, L. Evaluation of Ionic Liquid Gas Chromatography Stationary Phases for the Separation of Polychlorinated Biphenyls. *J. Chromatogr. A* **2017**, *1559*, 156–163.
- (22) Anderson, J. L.; Armstrong, D. W. High-Stability Ionic Liquids. A New Class of Stationary Phases for Gas Chromatography. *Anal. Chem.* **2003**, *75* (18), 4851–4858.
- (23) Anderson, J. L.; Ding, R.; Ellern, A.; Armstrong, D. W. Structure and Properties of High Stability Geminal Dicationic Ionic Liquids. *J. Am. Chem. Soc.* **2005**, *127*, 593–604.
- (24) Patil, R. A.; Talebi, M.; Xu, C.; Bhawal, S. S.; Armstrong, D. W. Synthesis of Thermally Stable Geminal Dicationic Ionic Liquids and Related Ionic Compounds: An Examination of Physicochemical Properties by Structural Modification. *Chem. Mater* **2016**, *28*, 4315–4323.

- (25) Maton, C.; De Vos, N.; Stevens, C. V. Ionic Liquid Thermal Stabilities: Decomposition Mechanisms and Analysis Tools. *Chem. Soc. Rev.* **2013**, *42* (13), 5963–5977.
- (26) Patil, R. A.; Talebi, M.; Berthod, A.; Armstrong, D. W. Dicationic Ionic Liquid Thermal Decomposition Pathways. *Anal. Bioanal. Chem.* **2018**, *410* (19), 4645–4655.
- (27) Rabideau, B. D.; West, K. N.; Davis, J. H. Making Good on a Promise: Ionic Liquids with Genuinely High Degrees of Thermal Stability. *Chem. Commun.* **2018**, *54* (40), 5019–5031.
- (28) Scheuermeyer, M.; Kusche, M.; Agel, F.; Schreiber, P.; Maier, F.; Steinrück, H.-P.; Davis, J. H.; Heym, F.; Jess, A.; Wasserscheid, P. Thermally Stable Bis(Trifluoromethylsulfonyl)Imide Salts and Their Mixtures. *New J. Chem.* **2016**, *40* (8), 7157–7161.
- (29) Siu, B.; Cassity, C. G.; Benchea, A.; Hamby, T.; Hendrich, J.; Strickland, K. J.; Wierzbicki, A.; Sykora, R. E.; Salter, E. A.; O'Brien, R. A.; et al. Thermally Robust: Triarylsulfonium Ionic Liquids Stable in Air for 90 Days at 300 °C. *RSC Adv.* **2017**, *7* (13), 7623–7630.
- (30) James, A. T. Determination of the Degree of Unsaturation of Long Chain Fatty Acids by Gas-Liquid Chromatography. *J. Chromatogr. A* **1959**, *2*, 552–561.
- (31) Liang, F.; Lu, M.; Birch, M. E.; Keener, T. C.; Liu, Z. Determination of Polycyclic Aromatic Sulfur Heterocycles in Diesel Particulate Matter and Diesel Fuel by Gas Chromatography with Atomic Emission Detection. *J. Chromatogr. A* **2006**, *1114* (1), 145–153.
- (32) Mottier, P.; Parisod, V.; Turesky, R. J. Quantitative Determination of Polycyclic Aromatic Hydrocarbons in Barbecued Meat Sausages by Gas Chromatography Coupled to Mass Spectrometry. *J. Agric. Food Chem.* **2000**, *48*, 1160–1166.
- (33) Zhang, C.; Park, R. A.; Anderson, J. L. Crosslinked Structurally-Tuned Polymeric Ionic Liquids as Stationary Phases for the Analysis of Hydrocarbons in Kerosene and Diesel Fuels by Comprehensive Two-Dimensional Gas Chromatography. *J. Chromatogr. A* **2016**, *1440*, 160–171.
- (34) Betts, T. J. Comparison of Four Liquid Crystal Stationary Phases Used above and below Their Melting Point Temperatures for the Gas Chromatography of Some Volatile Oil Constituents. *J. Chromatogr. A* **1991**, *588* (1–2), 231–237.
- (35) Denis, E. H.; Toney, J. L.; Tarozo, R.; Anderson, R. S.; Roach, L. D.; Huang, Y. Polycyclic Aromatic Hydrocarbons (PAHs) in Lake Sediments Record Historic Fire Events: Validation Using HPLC-Fluorescence Detection. *Org. Geochem.* **2012**, *45*, 7–17.
- (36) Shi, Y.; Wu, H.; Wang, C.; Guo, X.; Du, J.; Du, L. Determination of Polycyclic Aromatic Hydrocarbons in Coffee and Tea Samples by Magnetic Solid-Phase Extraction Coupled with HPLC–FLD. *Food Chem.* **2016**, *199*, 75–80.

- (37) Nisbet, I. C. T.; LaGoy, P. K. Toxic Equivalency Factors (TEFs) for Polycyclic Aromatic Hydrocarbons (PAHs). *Regul. Toxicol. Pharmacol.* **1992**, *16* (3), 290–300.
- (38) Ragonese, C.; Sciarrone, D.; Tranchida, P. Q.; Dugo, P.; Dugo, G.; Mondello, L.; Farmaco-Chimico, D. Evaluation of a Medium-Polarity Ionic Liquid Stationary Phase in the Analysis of Flavor and Fragrance Compounds. *Anal. Chem* **2011**, *83*, 7947–7954.
- (39) Harju, M.; Danielsson, C.; Haglund, P. Comprehensive Two-Dimensional Gas Chromatography of the 209 Polychlorinated Biphenyls. *J. Chromatogr. A* **2003**, *1019*, 111–126.
- (40) Falandysz, J.; Tanabe, S.; Tatsukawa, R. Most Toxic and Highly Bioaccumulative PCB Congeners in Cod-Liver Oil of Baltic Origin Processed in Poland during the 1970s and 1980s, Their TEQ-Values and Possible Intake. *Sci. Total Environ.* **1994**, *145* (3), 207–212.
- (41) Hunter, C. A.; Sanderson, J. M.; Vinter, J. G.; Chessari, G.; Adams, H.; Low, C. M. R.; Jimenez Blanco, J.-L. Quantitative Determination of Intermolecular Interactions with Fluorinated Aromatic Rings. *Chem. Eur. J.* **2002**, *7* (16), 3494–3503.
- (42) Abraham, M. H.; Poole, C. F.; Poole, S. K. Classification of Stationary Phases and Other Materials by Gas Chromatography. *J. Chromatogr. A* **1999**, *842* (1–2), 79–114.
- (43) Abraham, M. H. Scales of Solute Hydrogen-Bonding: Their Construction and Application to Physicochemical and Biochemical Processes. *Chem. Soc. Rev.* **1993**, *22*, 73–83.
- (44) Breitbach, Z. S.; Armstrong, D. W. Characterization of Phosphonium Ionic Liquids through a Linear Solvation Energy Relationship and Their Use as GLC Stationary Phases. *Anal. Bioanal. Chem.* **2008**, *390*, 1605–1617.
- (45) Hantao, L. W.; Najafi, A.; Zhang, C.; Augusto, F.; Anderson, J. L. Tuning the Selectivity of Ionic Liquid Stationary Phases for Enhanced Separation of Nonpolar Analytes in Kerosene Using Multidimensional Gas Chromatography. *Anal. Chem.* **2014**, *86*, 3717–3721.

Figures

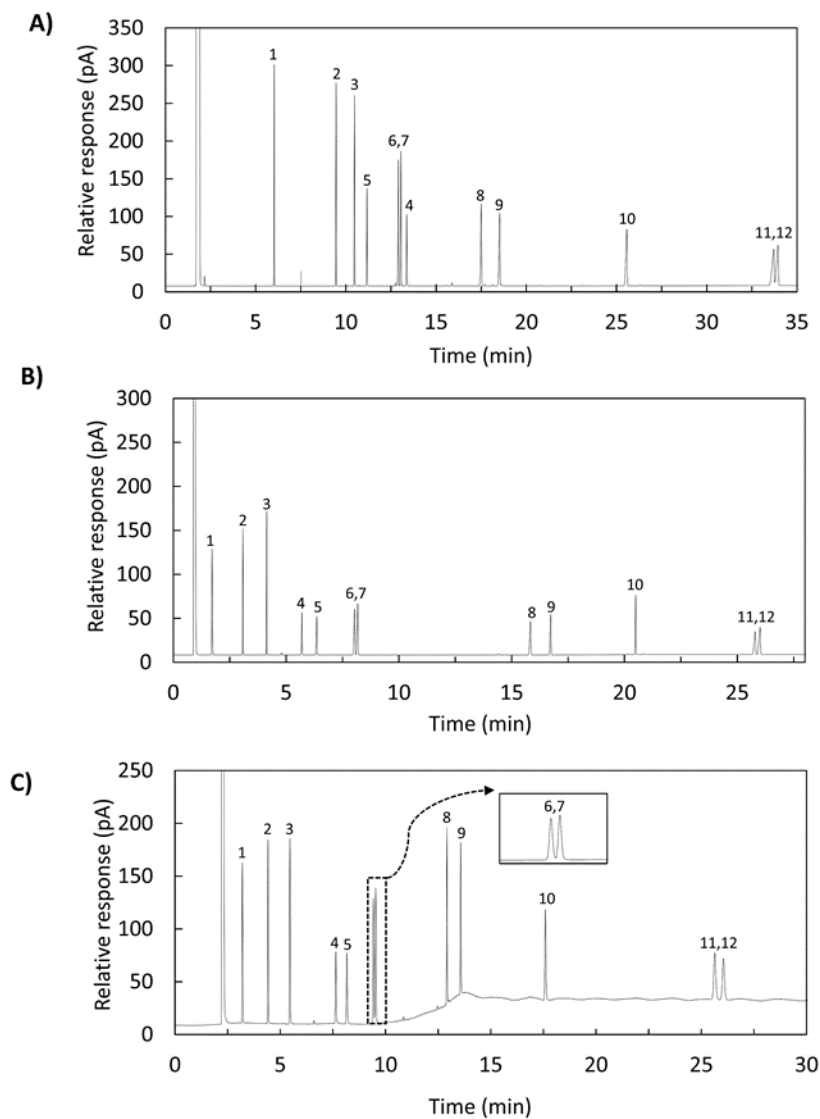


Figure 1. Chromatographic separation of PAHs on 3 different stationary phases. A) HP-5ms (30 m \times 250 μ m \times 0.25 μ m), B) SLB-ILPAH (20 m \times 180 μ m \times 0.05 μ m), C) IL 4 (30 m \times 250 μ m \times 0.20 μ m). Analytes: 1, naphthalene; 2, acenaphthene; 3, fluorene; 4, 5-bromoacenaphthene; 5, 2-nitronaphthalene; 6, phenanthrene; 7, anthracene; 8, fluoranthene; 9, pyrene; 10, benzo(a)fluoranthene; 11, benzo(b)fluoranthene and 12, benzo(k)fluoranthene. Separation conditions: A) initial, 95 $^{\circ}$ C for 2 min, 12 $^{\circ}$ C/min to 190 $^{\circ}$ C, 3 $^{\circ}$ C/min to 235 $^{\circ}$ C, 1.5 $^{\circ}$ C/min to 255 $^{\circ}$ C. B) 125-175 $^{\circ}$ C at 12 $^{\circ}$ C/min, hold for 4 min, 5 $^{\circ}$ C/min to 195 $^{\circ}$ C, hold for 3 min, 15 $^{\circ}$ C/min to 260 $^{\circ}$ C. C) initial, 200 $^{\circ}$ C for 1 min, 25 $^{\circ}$ C/min to 245 $^{\circ}$ C, hold for 7 min, 30 $^{\circ}$ C/min to 350 $^{\circ}$ C. Flow rate: 1 mL/min. Analyte concentration: 0.5 mg/mL.

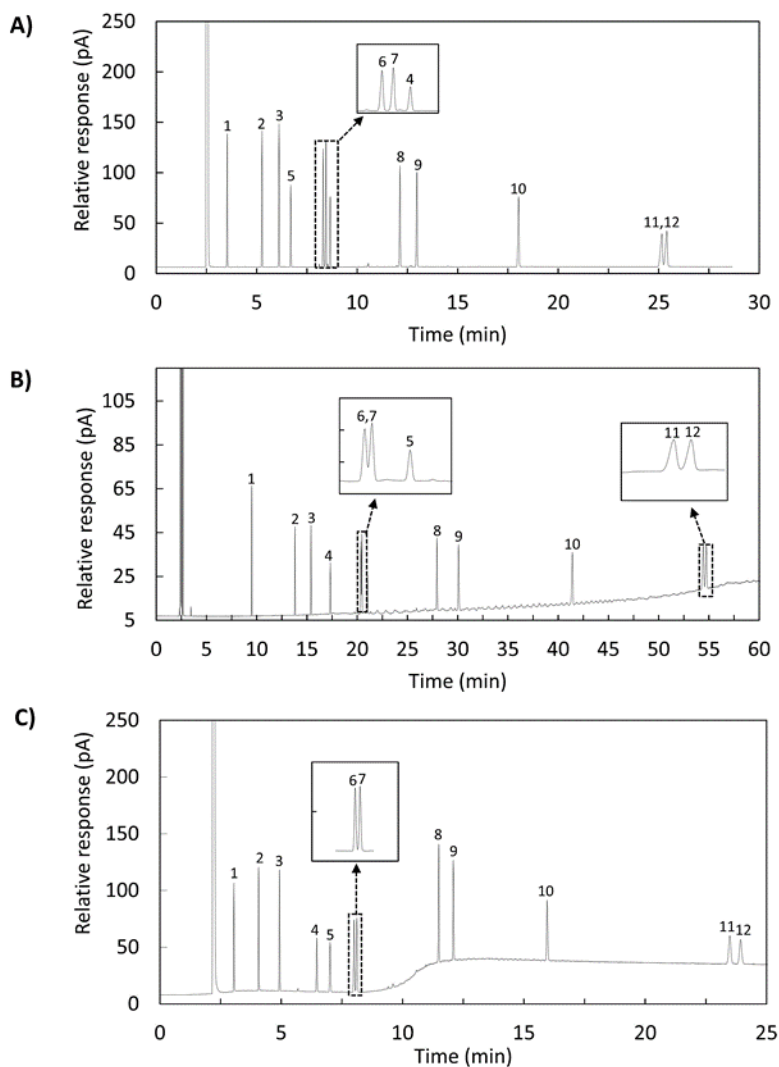


Figure 2. Chromatographic separation of PAHs on 3 different stationary phases. **A)** SLB-5ms (30 m \times 250 μ m \times 0.25 μ m), **B)** SPB-50 (30 m \times 250 μ m \times 0.25 μ m), **C)** IL 5 (30 m \times 250 μ m \times 0.20 μ m). Analytes: 1, naphthalene; 2, acenaphthene; 3, fluorene; 4, 5-bromoacenaphthene; 5, 2-nitronaphthalene; 6, phenanthrene; 7, anthracene; 8, fluoranthene; 9, pyrene; 10, benzo(a)fluoranthene; 11, benzo(b)fluoranthene and 12, benzo(k)fluoranthene. Separation conditions: **A)** 150-200 $^{\circ}$ C at 15 $^{\circ}$ C/min, hold for 1 min, 5 $^{\circ}$ C/min to 260 $^{\circ}$ C. **B)** 125-185 $^{\circ}$ C at 12 $^{\circ}$ C/min, held for 2 min, 10 $^{\circ}$ C/min to 220 $^{\circ}$ C, hold for 2 min, 1.5 $^{\circ}$ C/min to 250 $^{\circ}$ C. **C)** initial, 205 $^{\circ}$ C for 1 min, 25 $^{\circ}$ C/min to 260 $^{\circ}$ C, hold for 5 min, 30 $^{\circ}$ C/min to 330 $^{\circ}$ C. Flow rate: 1 mL/min. Analyte concentration: 0.5 mg/mL.

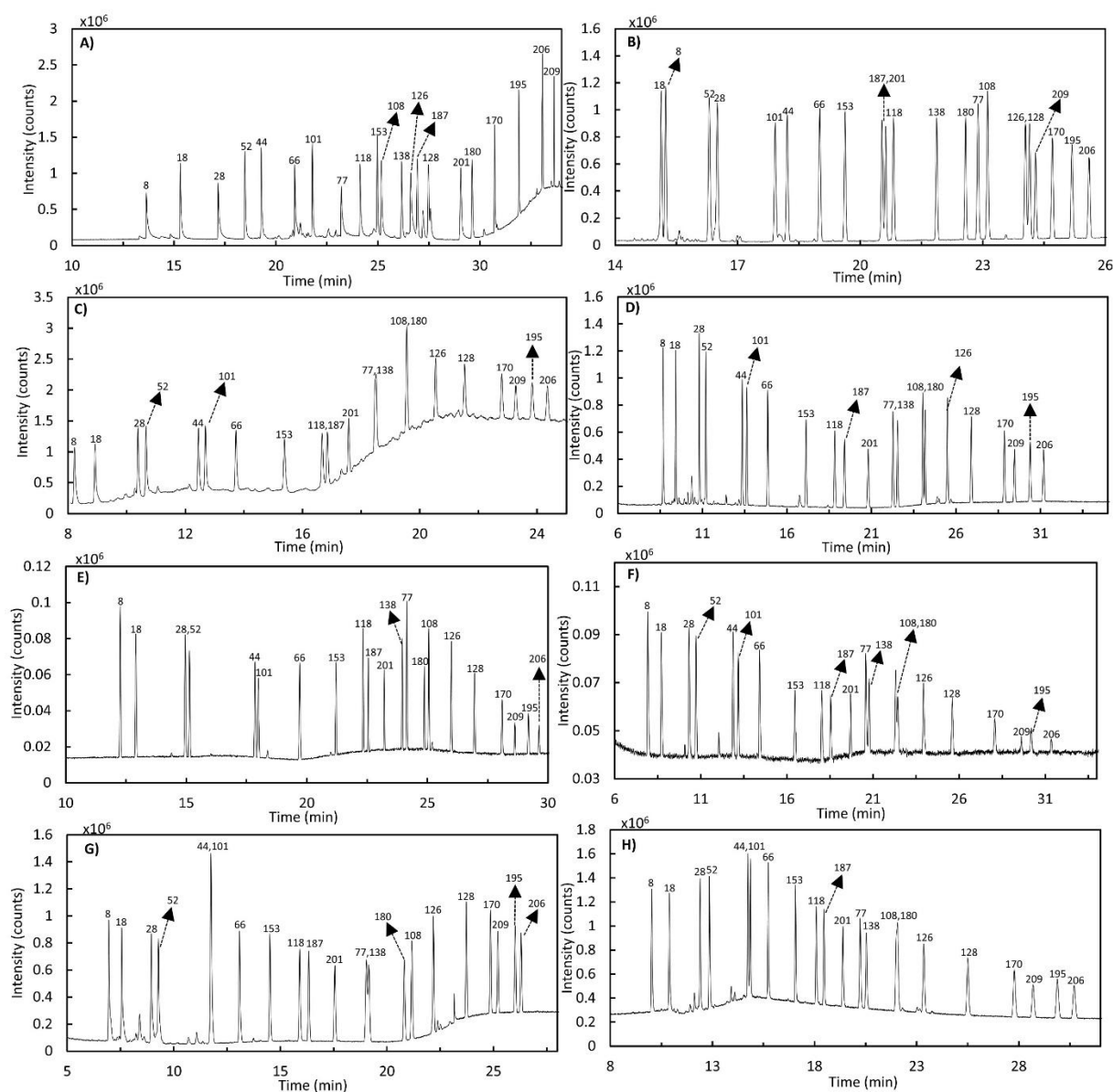


Figure 3. Chromatographic separation of 21 PCBs on eight columns. A) HP-5ms UI (30 m \times 250 μm \times 0.25 μm), B) SLB-IL111 (30 m \times 250 μm \times 0.20 μm), C) IL 1 (30 m \times 250 μm \times 0.20 μm), D) IL 2 (30 m \times 250 μm \times 0.20 μm), E) IL 3 (30 m \times 250 μm \times 0.20 μm), F) IL 4 (30 m \times 250 μm \times 0.20 μm), G) IL 5 (30 m \times 250 μm \times 0.20 μm), H) IL 6 (30 m \times 250 μm \times 0.20 μm). The temperature program was optimized for each column (see experimental section and Table S10 for each optimized temperature program). Separations were performed on an Agilent 7890B/5977A GC/MS system. Helium was used as the carrier gas at a flow rate of 1 mL/min. The injector temperatures were held at 250 $^{\circ}\text{C}$ and a split ratio of 5:1 was used. The MS was operated at 70 eV with electron ionization (EI) in SCAN mode. Refer to Table S2 for the corresponding name and chemical structure of the PCBs.

Tables

Table 1. Chemical structures of the high thermal stability ILs examined as stationary phases in this study

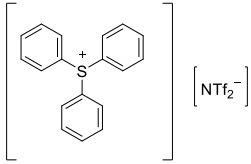
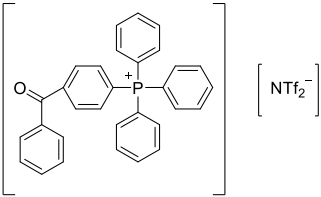
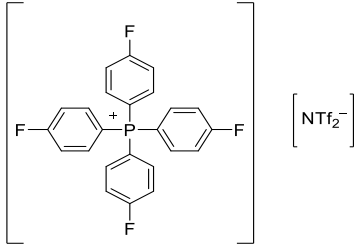
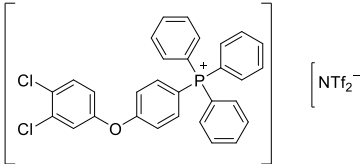
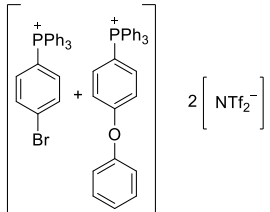
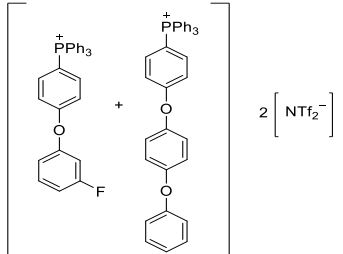
IL No.	Chemical Name of IL	Chemical Structure
1	Triphenylsulfonium bis[(trifluoromethyl)sulfonyl]imide	
2	(4-Benzoylphenyl)triphenylphosphonium bis[(trifluoromethyl)sulfonyl]imide	
3	Tetrakis(4-fluorophenyl)phosphonium bis[(trifluoromethyl)sulfonyl]imide	
4	(4-(3,4-Dichlorophenoxy)phenyl)triphenylphosphonium bis[(trifluoromethyl)sulfonyl]imide	
5	Mixture of (4-bromophenyl)triphenylphosphonium bis[(trifluoromethyl)sulfonyl]imide and (4- phenoxyphenyl)triphenylphosphonium bis[(trifluoromethyl)sulfonyl]imide	
6	Mixture of (4-(3- fluorophenoxy)phenyl)triphenylphosphonium bis[(trifluoromethyl)sulfonyl]imide and (4-(4- phenoxyphenoxy)phenyl)triphenylphosphonium bis[(trifluoromethyl)sulfonyl]imide	

Table 2. Studied IL-based stationary phases with their corresponding column dimensions, chromatographic efficiency, and thermal stability

Stationary Phase	Column Length (m)	Film Thickness (μm)	Efficiency ^a (plates/meter)	Thermal Stability ^b ($^{\circ}\text{C}$)
IL 1	30	0.20	3774	300
IL 2	30	0.20	3741	310
IL 3	30	0.20	4190	310
IL 4	30	0.20	4154	350
IL 5	30	0.20	4379	350
IL 6	30	0.20	4270	290

^a All columns were evaluated at 110 $^{\circ}\text{C}$ using naphthalene as the test probe to determine the chromatographic efficiency.

^b Thermal stability was determined by taking 5 m segments of each column and conditioning them for one hour at each temperature from 100 to 350 $^{\circ}\text{C}$ in 50 $^{\circ}\text{C}$ increments. The efficiency of each column was tested after each conditioning step (See Tables S4-S9).

Table 3. Comparison of chromatographic selectivity and resolution for five PCB analyte pairs on six IL-based columns and two commercial columns

Stationary phase	PCB 44/101			PCB 77/138			PCB 108/180			PCB 126/128			PCB 108/153		
	EO ^a	α^b	R_s	EO ^a	α^b	R_s	EO ^a	α^b	R_s	EO ^a	α^b	R_s	EO ^a	α^b	R_s
HP-5ms UI	44/101	1.13	32.57	77/138	1.13	29.63	108/180	1.18	49.11	126/128	1.03	8.26	153/108	1.01	2.26
SLB-IL111	101/44	1.01	3.52	138/77	1.04	13.44	180/108	1.02	7.37	126/128	1.01	1.27	153/108	1.18	45.71
IL 1	44/101	1.02	2.69	77/138	1.00 ^c	0 ^c	108/180	1.00 ^c	0 ^c	126/128	1.04	9.80	153/108	1.27	39.05
IL 2	44/101	1.02	2.82	77/138	1.01	2.23	108/180	1.01	1.38	126/128	1.05	11.90	153/108	1.40	60.42
IL 3	44/101	1.01	1.66	138/77	1.01	3.06	180/108	1.01	2.89	126/128	1.03	12.66	153/108	1.18	54.75
IL 4	44/101	1.02	2.83	77/138	1.01	1.41	108/180	1.01	1.08	126/128	1.07	11.24	153/108	1.35	46.30
IL 5	44/101	1.00 ^c	0 ^c	77/138	1.01	0.97	180/108	1.04	2.88	126/128	1.07	14.94	153/108	1.46	68.64
IL 6	44/101	1.01	1.43	77/138	1.02	2.07	108/180	1.00 ^c	0 ^c	126/128	1.09	13.05	153/108	1.29	36.34

Supplemental

Table S1. Chemical structures and boiling points of the 12 selected PAHs separated in this study

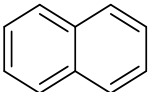
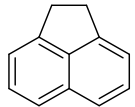
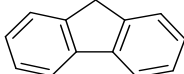
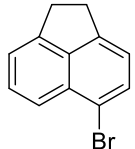
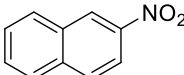
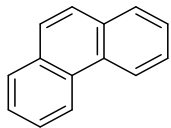
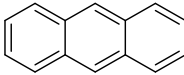
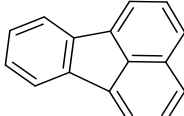
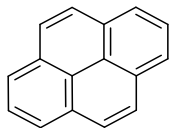
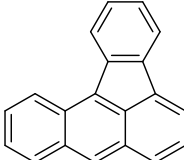
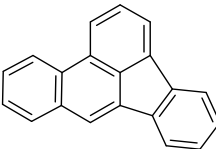
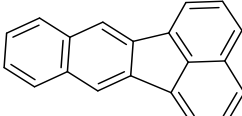
Name	Chemical Structure	Boiling Point (°C)
Naphthalene		218 (760 mmHg)
Acenaphthene		279 (760 mmHg)
Fluorene		298 (760 mmHg)
5-Bromoacenaphthene		335 (760 mmHg)
2-Nitronaphthalene		312.5 (734.4 mmHg)
Phenanthrene		340 (760 mmHg)
Anthracene		354 (760 mmHg)
Fluoranthene		375 (760 mmHg)
Pyrene		404 (760 mmHg)
Benzo(a)fluoranthene		481 (760 mmHg)
Benzo(b)fluoranthene		481 (760 mmHg)
Benzo(k)fluoranthene		480 (760 mmHg)

Table S2 Name and chemical structures of 21 PCBs along with their specific congener subjected to separation in this study

PCB ^a	Name	Chemical Structure
8	2,4'-dichlorobiphenyl	
18	2,2',5-trichlorobiphenyl	
28	2,4,4'-trichlorobiphenyl	
52	2,2',5,5'-tetrachlorobiphenyl	
44	2,2',3,5'-tetrachlorobiphenyl	
66	2,3',4,4'-tetrachlorobiphenyl	
101	2,2',4,5,5'-pentachlorobiphenyl	
77	3,3',4,4'-tetrachlorobiphenyl	
118	2,3',4,4',5-pentachlorobiphenyl	
153	2,2',4,4',5,5'-hexachlorobiphenyl	
108	2,3,3',4,4'-pentachlorobiphenyl	
138	2,2',3,4,4',5'-hexachlorobiphenyl	
126	3,3',4,4',5-pentachlorobiphenyl	
187	2,2',3,4',5,5',6-heptachlorobiphenyl	
128	2,2',3,3',4,4',-hexachlorobiphenyl	

Table S2 continued

PCB ^a	Name	Chemical Structure
201	2,2',3,3',4,5',6,6'-octachlorobiphenyl	
180	2,2',3,4,4',5,5'-heptachlorobiphenyl	
170	2,2',3,3',4,4',5-heptachlorobiphenyl	
195	2,2',3,3',4,4',5,6-octachlorobiphenyl	
206	2,2',3,3',4,4',5,5',6-nonachlorobiphenyl	
209	2,2',3,3',4,4',5,5',6,6'-decachlorobiphenyl	

^aThe name of each of the congener is specific to the total number of chlorine substituents and the position of each chlorine atom.

Table S3. List of all probe molecules and their corresponding solute descriptors used to characterize IL-based stationary phases employing the solvation parameter model

Probe molecule	E	S	A	B	L
Acetic acid	0.265	0.65	0.61	0.44	1.75
Acetophenone	0.818	1.01	0	0.48	4.501
Aniline	0.955	0.96	0.26	0.41	3.934
Benzaldehyde	0.82	1	0	0.39	4.008
Benzene	0.61	0.52	0	0.14	2.786
Benzonitrile	0.742	1.11	0	0.33	4.039
Benzyl alcohol	0.803	0.87	0.33	0.56	4.221
Bromoethane	0.366	0.4	0	0.12	2.62
1-Bromooctane	0.339	0.4	0	0.12	5.09
1-Butanol	0.224	0.42	0.37	0.48	2.601
Butyraldehyde	0.187	0.65	0	0.45	2.27
2-Chloroaniline	1.033	0.92	0.25	0.31	4.674
1-Chlorobutane	0.21	0.4	0	0.1	2.722
1-Chlorohexane	0.201	0.4	0	0.1	3.777
1-Chlorooctane	0.191	0.4	0	0.1	4.772
<i>p</i> -Cresol	0.82	0.87	0.57	0.31	4.312
Cyclohexanol	0.46	0.54	0.32	0.57	3.758
Cyclohexanone	0.403	0.86	0	0.56	3.792
1,2-Dichlorobenzene	0.872	0.78	0	0.04	4.518
<i>N,N</i> -Dimethylformamide	0.367	1.31	0	0.74	3.173
1,4-Dioxane	0.329	0.75	0	0.64	2.892
Ethyl acetate	0.106	0.62	0	0.45	2.314
Ethyl benzene	0.613	0.51	0	0.15	3.778
1-Iodobutane	0.628	0.4	0	0.15	4.13
Methyl caproate	0.067	0.6	0	0.45	3.844
Naphthalene	1.34	0.92	0	0.2	5.161
Nitrobenzene	0.871	1.11	0	0.28	4.557
1-Nitropropane	0.242	0.95	0	0.31	2.894
1-Octanol	0.199	0.42	0.37	0.48	4.619
Octylaldehyde	0.16	0.65	0	0.45	4.361
1-Pentanol	0.219	0.42	0.37	0.48	3.106
2-Pentanone	0.143	0.68	0	0.51	2.755
Ethyl phenyl ether	0.681	0.7	0	0.32	4.242
Phenol	0.805	0.89	0.6	0.3	3.766
Propionitrile	0.162	0.9	0.02	0.36	2.082
Pyridine	0.631	0.84	0	0.52	3.022
Pyrrole	0.613	0.73	0.41	0.29	2.865
Toluene	0.601	0.52	0	0.14	3.325
<i>m</i> -Xylene	0.623	0.52	0	0.16	3.839
<i>o</i> -Xylene	0.663	0.56	0	0.16	3.939
<i>p</i> -Xylene	0.613	0.52	0	0.16	3.839

Table S3 continued

Probe molecule	E	S	A	B	L
2-Propanol	0.212	0.36	0.33	0.56	1.764
2-Nitrophenol	1.015	1.05	0.05	0.37	4.76
1-Bromohexane	0.349	0.4	0	0.12	4.13
Propionic acid	0.233	0.65	0.6	0.45	2.29
1-Decanol	0.191	0.42	0.37	0.48	5.628

Data obtained from reference[1].

Table S4. Chromatographic performance of IL **1** using naphthalene as the probe molecule

Temperature (°C)	Trial	Retention time (min)	Peak width (min)	Efficiency (plates/meter)
100	1	3.89	0.072	3217
	2	3.89	0.074	3078
	3	3.83	0.070	3289
	Std	0.03	0.002	107
150	1	3.80	0.063	2954
	2	3.80	0.073	3012
	3	3.80	0.068	3466
	Std	0.02	0.005	280
200	1	3.76	0.073	2950
	2	3.80	0.071	3188
	3	3.79	0.064	3892
	Std	0.02	0.005	490
250	1	3.69	0.072	2941
	2	3.73	0.064	3646
	3	3.74	0.071	3087
	Std	0.03	0.004	372
270	1	3.59	0.069	2670
	2	3.62	0.070	2942
	3	3.64	0.064	3627
	Std	0.02	0.004	493
290	1	3.41	0.037	3187
	2	3.44	0.064	3193
	3	3.45	0.073	2511
	Std	0.02	0.019	392
310	1	3.23	0.069	2423
	2	3.24	0.067	2571
	3	3.22	0.065	2746
	Std	0.01	0.002	162
330	1	2.78	0.072	1650
	2	2.83	0.071	1750
	3	2.85	0.071	1783
	Std	0.04	0.001	69
350	1	2.34	0.073	1128
	2	2.45	0.077	1125
	3	2.44	0.074	1191
	Std	0.06	0.002	37

Experimental condition: 100 °C isothermal separation; flow rate: 1 mL/min. Injection volume: 1 µL.

Table S5. Chromatographic performance of IL **2** using naphthalene as the probe molecule

Temperature (°C)	Trial	Retention time (min)	Peak width (min)	Efficiency (plates/meter)
100	1	3.37	0.070	2545
	2	3.37	0.072	2408
	3	3.36	0.070	2532
	Std	0.01	0.001	76
150	1	3.30	0.065	2818
	2	3.30	0.068	2582
	3	3.30	0.065	2799
	Std	0.01	0.002	131
200	1	3.23	0.065	2768
	2	3.26	0.072	2296
	3	3.26	0.063	2926
	Std	0.02	0.004	328
250	1	3.11	0.068	2342
	2	3.19	0.063	2873
	3	3.21	0.068	2488
	Std	0.06	0.003	274
270	1	3.11	0.066	2488
	2	3.14	0.064	2715
	3	3.14	0.066	2506
	Std	0.02	0.001	126
290	1	3.04	0.064	2480
	2	3.07	0.065	2456
	3	3.08	0.066	2444
	Std	0.02	0.001	18
310	1	2.96	0.064	2548
	2	2.95	0.061	2625
	3	2.92	0.061	2403
	Std	0.02	0.002	113
330	1	2.73	0.063	2091
	2	2.76	0.059	2395
	3	2.78	0.063	2168
	Std	0.03	0.002	158
350	1	2.38	0.058	1840
	2	2.41	0.061	1738
	3	2.43	0.061	1769
	Std	0.03	0.002	52

Experimental condition: 100 °C isothermal separation; flow rate: 1 mL/min. Injection volume: 1 µL.

Table S6. Chromatographic performance of IL **3** using naphthalene as the probe molecule

Temperature (°C)	Trial	Retention time (min)	Peak width (min)	Efficiency (plates/meter)
110	1	2.54	0.075	1270
	2	2.54	0.080	1108
	3	2.53	0.082	1091
	Std	0.01	0.004	99
150	1	2.59	0.083	1073
	2	2.56	0.085	1005
	3	2.59	0.084	1040
	Std	0.02	0.001	34
200	1	2.62	0.092	895
	2	2.63	0.095	842
	3	2.63	0.093	888
	Std	0.01	0.002	29
250	1	2.65	0.096	840
	2	2.63	0.097	823
	3	2.19	0.094	893
	Std	0.26	0.002	37
270	1	2.67	0.097	844
	2	2.63	0.098	806
	3	2.67	0.100	792
	Std	0.02	0.002	27
290	1	2.69	0.104	736
	2	2.66	0.105	713
	3	2.65	0.103	733
	Std	0.02	0.001	13
310	1	2.71	0.116	733
	2	2.71	0.114	713
	3	2.71	0.117	593
	Std	0.01	0.002	76
330	1	2.69	0.204	220
	2	2.82	0.225	173
	3	2.84	0.223	179
	Std	0.08	0.012	26
350	1	6.90	1.64	20
	2	7.11	1.70	19
	3	7.09	1.64	21
	Std	0.12	0.04	1

Experimental condition: 110 °C isothermal separation; flow rate: 1 mL/min. Injection volume: 1 µL.

Table S7. Chromatographic performance of IL **4** using naphthalene as the probe molecule

Temperature (°C)	Trial	Retention time (min)	Peak width (min)	Efficiency (plates/meter)
100	1	5.06	0.079	4511
	2	5.06	0.088	4502
	3	5.03	0.085	3894
	Std	0.02	0.004	354
150	1	4.90	0.086	3680
	2	4.90	0.087	3575
	3	4.90	0.081	4152
	Std	0.01	0.003	307
200	1	4.84	0.082	3899
	2	4.88	0.094	3023
	3	4.90	0.086	3626
	Std	0.03	0.006	448
250	1	4.81	0.080	4007
	2	4.85	0.083	3820
	3	4.87	0.082	3939
	Std	0.03	0.001	95
270	1	4.73	0.085	3411
	2	4.80	0.081	3887
	3	4.83	0.081	3902
	Std	0.05	0.002	279
290	1	4.70	0.083	3534
	2	4.75	0.085	3504
	3	4.77	0.083	3683
	Std	0.04	0.001	96
310	1	4.78	0.090	3157
	2	4.78	0.088	3305
	3	4.78	0.091	3055
	Std	0.01	0.002	126
330	1	4.47	0.079	4431
	2	4.56	0.091	2783
	3	4.59	0.090	2915
	Std	0.06	0.007	916
350	1	4.25	0.086	2683
	2	4.32	0.083	2968
	3	4.34	0.085	2876
	Std	0.04	0.002	145

Experimental condition: 100 °C isothermal separation; flow rate: 1 mL/min. Injection volume: 1 µL.

Table S8. Chromatographic performance of IL **5** using naphthalene as the probe molecule

Temperature (°C)	Trial	Retention time (min)	Peak width (min)	Efficiency (plates/meter)
100	1	5.06	0.079	4511
	2	5.06	0.088	4502
	3	5.03	0.085	3894
	Std	0.02	0.005	354
150	1	4.90	0.086	3680
	2	4.90	0.087	3575
	3	4.90	0.081	4152
	Std	0.01	0.003	307
200	1	4.84	0.082	3899
	2	4.88	0.094	3023
	3	4.90	0.086	3626
	Std	0.03	0.006	448
250	1	4.81	0.080	4007
	2	4.85	0.083	3820
	3	4.87	0.082	3939
	Std	0.03	0.001	95
270	1	4.73	0.085	3411
	2	4.80	0.081	3887
	3	4.83	0.081	3902
	Std	0.05	0.002	279
290	1	4.70	0.083	3534
	2	4.75	0.085	3504
	3	4.77	0.083	3683
	Std	0.04	0.001	96
310	1	4.78	0.090	3157
	2	4.78	0.088	3305
	3	4.78	0.091	3055
	Std	0.01	0.002	126
330	1	4.47	0.079	4431
	2	4.56	0.091	2783
	3	4.59	0.090	2915
	Std	0.06	0.007	916
350	1	4.25	0.086	2683
	2	4.32	0.083	2968
	3	4.34	0.085	2876
	Std	0.04	0.002	145

Experimental condition: 100 °C isothermal separation; flow rate: 1 mL/min. Injection volume: 1 µL.

Table S9. Chromatographic performance of IL **6** using naphthalene as the probe molecule

Temperature (°C)	Trial	Retention time (min)	Peak width (min)	Efficiency (plates/meter)
100	1	3.87	0.096	1792
	2	3.86	0.099	1674
	3	3.86	0.099	1684
	Std	0.01	0.002	65
150	1	3.9	0.096	1832
	2	3.9	0.099	1803
	3	3.8	0.095	1780
	Std	0.03	0.002	26
200	1	3.77	0.093	1835
	2	3.84	0.094	1850
	3	3.84	0.091	1981
	Std	0.04	0.002	80
250	1	3.83	0.095	1670
	2	3.75	0.097	1814
	3	3.83	0.095	1803
	Std	0.04	0.001	80
270	1	3.63	0.080	2290
	2	3.63	0.088	1901
	3	3.63	0.084	2066
	Std	0.01	0.004	195
290	1	3.48	0.089	1710
	2	3.57	0.089	1774
	3	3.59	0.092	1678
	Std	0.06	0.002	49
310	1	3.51	0.095	1495
	2	3.47	0.098	1390
	3	3.51	0.097	1442
	Std	0.02	0.001	53
330	1	3.35	0.106	1108
	2	3.40	0.100	1271
	3	3.42	0.109	1074
	Std	0.04	0.004	105
350	1	3.19	0.121	764
	2	3.25	0.131	676
	3	3.25	0.120	815
	Std	0.04	0.006	70

Experimental condition: 100 °C isothermal separation; flow rate: 1 mL/min. Injection volume: 1 µL.

CHAPTER 3. CHARACTERIZING THE SOLVATION INTERACTIONS OF DEEP EUTECTIC SOLVENTS BY ABRAHAM SOLVATION PARAMETER MODEL

Muhammad Qamar Farooq,^a Gabriel A. Odugbesi,^a Nabeel Mujtaba Abbasi,^a Emily A. Smith,^a Jacob W. Petrich,^a Xueyu Song,^a Jared L. Anderson^{a,*}

^aDepartment of Chemistry, Iowa State University, Ames, Iowa 50011, USA

Abstract

Deep eutectic solvents (DESs) are a relatively new class of ionic solvents consisting of a hydrogen bond donor (HBD) and a hydrogen bond acceptor (HBA). Hydrogen bonding is a principal driving force behind the formation of liquid eutectic mixtures with melting points lower than that of their individual components. Characteristics such as low toxicity, low cost, low vapor pressure, and simple and green synthesis make them suitable alternatives to ionic liquids (ILs). ILs, on the other hand, have lower biodegradability as well as relatively higher cost and toxicity as compared to DESs. DESs have been applied in fields ranging from analytical extractions to organic synthesis as well as task-specific applications like carbon dioxide capture. However, very little is understood regarding their physiochemical properties and solvation interactions. In this work, a broad range of these compounds are characterized by the Abraham solvation parameter model. This model allows for study of the solvation properties of DESs and the effects of varying structural components on the system constants. The model uses a linear free energy relationship to characterize liquid/gas phase interactions between solute molecules and the gas chromatographic stationary phase.

Introduction

Deep eutectic solvents (DES) are homogenous mixtures formed through the combination of a hydrogen bond donor (HBD) and hydrogen bond acceptor (HBA).¹⁻³ This combination results in

a lower melting point of the DES than both individual components.⁴ The majority of HBAs used to form DES are quaternary ammonium or phosphonium salts,^{5,6} while HBDs are typically comprised of metal halides, carbohydrates, amides, alcohols, or carboxylic acids.³ DES have been applied in numerous applications such as solvents in the extraction of metals,⁷ bio-catalysis,⁸⁻¹⁰ carbon dioxide capture,^{11,12} extraction and purification of bioactive compounds,¹³ biodiesel production,^{14,15} and desulfurization of fuels.¹⁶⁻¹⁹ Furthermore, DES have also been used for electrodeposition of metals and structure-directing agents for the template-assisted synthesis of porous frameworks.²⁰⁻²²

DES have garnered considerable attention over the last couple of decades as potential alternatives to ionic liquids (ILs). ILs are molten organic salts comprised of an anion and a cation with melting points below 100 °C. Like ILs, DES also possess negligible vapor pressure and a broad liquid range. The physiochemical properties of DES can be easily controlled by tailoring the chemical structure of the HBA/HBD, as well as their relative molar ratio.^{23,24} DES hydrophobicity and hydrophilicity can be modulated by varying the alkyl chain length and functional group substituents within the HBDs and HBAs.^{5,25,11} Moreover, the low cost of starting materials and a solventless and purification-free synthesis, makes DES more advantageous than ILs.^{6,26} The biodegradability and toxicity of DES can be easily controlled by carefully choosing the HBAs and HBDs. DES comprised of choline chloride and glycerol possess high biodegradability and low toxicity,^{27,28} while those containing metal halides such as ZnCl₂ are considered toxic.²⁹

An understanding of DES solvation interactions is critical to explore their potential uses and fine-tune their physiochemical properties for specific applications. Until now, only empirical polarity scales based upon solvatochromic probes have been used to characterize DES. Reichardt's polarity index, based on the negative solvatochromism of Betaine dye 30 (2,6-diphenyl-4-(2,4,6-

triphenyl-pyridinium-1-yl)phenolate), is widely used for measuring the polarity of many solvents including DESs and ILs.^{30,31} Normalized solvent polarity parameter (E_TN) can be easily obtained from the maximum of absorption of dye in the solvent under study. Since E_TN is a single polarity parameter and results in an average value derived from all the solvation interactions (hydrogen bonding, dispersive, dipolarity/polarizability, $n-\pi/\pi-\pi$) between the probe and DES, these polarity values are often unable to differentiate between structurally diverse compounds. Similarly, Kamlet-Taft parameters have also been used to characterize the solvation properties of DES. Various solvatochromic probes including Betaine dye 30, 4-nitroaniline, and *N,N*-diethyl-4-nitroaniline have been used to evaluate the hydrogen bond donating ability (α), hydrogen bond accepting ability (β), and polarity/polarizability (π^*).^{32,33} The solvatochromic shift of different probes is used to separately quantify various solvation interactions, as compared to the single parameter of Reichardt's polarity index. Although the addition of two more solvatochromic probes in the Kamlet-Taft parameter improves the study of solute-solvent interactions compared to Reichardt's polarity index, there is no single probe molecule or macroscopic physiochemical parameter to provide a suitable and comprehensive scale of solvent polarity of these DES.³⁴ Moreover, the presence of acidic HBDs is known to interfere with the solvatochromic behavior of betaine dye 30 due to its zwitterionic nature.³⁵

However, the limited sensitivity of these methods makes it challenging to accurately characterize DES. Oftentimes, solvatochromic methods suggest that DES possessing different HBA and HBD appear to have similar polarity values. Additionally, the shift in absorption spectra of dyes (used to derive the empirical polarity values) is limited, which makes it challenging to deconvolute subtle differences of chemical structure on the solvation properties leading to varying extraction efficiencies, catalytic activities, and solubilities of various molecules.²³ The minute

polarity differences characterized by solvatochromic approaches are unable to convincingly explain the performance of different DES in various applications including various extractions and catalytic applications. DES have been employed for the extraction of Cynaropicrin from *Cynara cardunuculus* L. leaves, where the extractions efficiencies were compared using DES composed of butanoic acid as HBD mixed with tetrabutylammonium bromide ($[N_{4444}^+][Br^-]$) as the HBA at two different ratios.³⁶ It was observed that the 1 to 2 molar ratio of HBA to HBD displayed extraction efficiencies approximately ten times higher compared to one equivalent of the HBD. Despite significance difference in extraction efficiencies upon varying the relative ratio of HBA to HBD, the β value (hydrogen bond accepting ability) in the Kamlet-Taft parameters for $[N_{4444}^+][Br^-]$ with butanoic acid was found be 0.81, 0.84 and 0.82 for relative HBA: HBD ratios of 1:2, 1:1, 2:1, respectively.²³ Similarly, the solubility of Acetaminophen in choline chloride with two equivalents of ethylene glycol is double than that of choline chloride with two equivalents of glycerol although their E_{TN} values (0.83 and 0.84, respectively) suggest similar solvation capabilities.³⁷⁻³⁹ Mokhtarpour et al., have also reported that Piroxicam (anti-inflammatory drug) is ten times more soluble in choline chloride-based DES with urea ($E_{TN} = 0.81$) as the HBD as compared to glycerol ($E_{TN} = 0.83$) as the HBD.^{37,38}

The limited understanding of the solvation properties of DES makes it strenuous to understand their potential applications. Therefore, there is a need for a more sensitive and universal technique to study their solvation properties. Previously, inverse gas chromatography (GC) has been employed to characterize the multiple solvation interactions of complex solvents such as ILs.⁴⁰ Several ILs have been studied using this model to understand the role of structural differences on their solvation properties and catalytic activities.⁴⁰ In this approach, the stationary phase is composed of the material of interest and retention of individual probe molecules capable

of undergoing multiple interactions with are analyzed.⁴¹ This approach is beneficial as it requires very small amounts of sample (15-20 mg). Temperature can also be easily modulated to understand its effect on the solvation properties of DES, such as an increase or decrease in the extent of hydrogen bonding with solute molecules.³⁴ DES solvation interactions can be characterized using the Abraham solvation parameter model. This model quantitatively measures the interactions of probe molecules with the solvent via inverse gas chromatography. The Abraham solvation parameter model is a linear free energy relationship that describes the gas/liquid phase molecular interactions based on the retention of probe molecules.^{42,43}

$$\text{Log } k = c + eE + sS + aA + bB + lL \quad (1)$$

As shown in equation 1, k refers to the retention factor of each probe molecule on the DES stationary phases at three temperatures. The solute descriptors (E , S , A , B , and L) were experimentally determined by Abraham et al. and are defined as: E , the excess molar refraction calculated from the solute's refractive index; S , the solutes dipolarity/polarizability; A , the solute hydrogen bond acidity; B , the solute hydrogen bond basicity; and L , the solute gas-hexadecane partition coefficient at 298. A list of the interaction parameters for the probe molecules chosen are shown in Table S1. Each solute contains different functional groups such as acidic, basic, aromatic, electron-withdrawing, and electron-donating which enable them to undergo various solute-solvent interactions. The magnitude of each interaction is measured by a multi-linear regression analysis. This model has been utilized to characterize the solvation interaction of several chiral compounds,⁴⁴ molten salts,^{45,46} ionic liquids,^{40,47,48} and a number of other solvents by gas chromatography.^{44,49}

In this study, a series of twenty DES including phosphonium and ammonium halide-based HBAs ($[P_{66614}^+][Cl^-]$, $[P_{4444}^+][Cl^-]$, $[P_{Al(Ph)_3}^+][Br^-]$, $[N_{4444}^+][Br^-]$, $[N_{4444}^+][Cl^-]$, $[N_{3333}^+][Cl^-]$, and

[N₂₂₂₂⁺][Cl⁻]) alongside a wide variety of carboxylic and sulfonic acid-based HBDs were characterized. These DES were applied as GC stationary phases to classify their molecular interactions. This study comprehensively examines the effect of pK_a of HBD, chain length of HBD, number of carboxyl functional groups in HBD, and relative molar ratio of HBA to HBD as well as the effect of varying anion and cation in HBA along with alkyl chain length of HBD on the solvation properties of DES. This knowledge can give us insight into enhancing the solvation as well as the extraction efficiencies of DES indifferent chemical processes and significantly decreasing the time required for finding the optimal DES for targeted applications. Such as DES possessing the capability to have extensive hydrogen bonding with solute molecules can be more beneficial towards desulfurization of fuels since they can undergo hydrogen bonding between sulfide groups of the contaminants.^{17,50} Moreover, thousands of possible combinations of DES make the trial and error process very tedious, so by the exploration of their molecular interactions, powerful solvents capable of unique properties can be designed for task-specific applications.

Materials and methods

Materials

Butyraldehyde (99%), 1-chlorobutane (99%), ethyl acetate (99.5%), methyl caproate (99%), naphthalene (99%), cyclopentanol (99%), nitromethane (99%), malonic acid (Mal. A., 99%), and 2-nitrophenol (99%) were purchased from Acros Organics (Morris Plains, NJ, USA). Bromoethane (98%) and l-lactic acid (Lac. A., 98%) were purchased from Alfa Aesar (Ward Hill, MA, USA). Ethyl benzene was purchased from Eastman Kodak Company (Rochester, NJ, USA). Acetic acid (99.9%), *N,N*-dimethylformamide (99.9%), 1-hexanol (98%), cycloheptanol (98%) and toluene (99.8%) were purchased from Fisher Scientific (Pittsburgh, PA, USA). 2-chloroaniline (98%), *p*-cresol (99%), *o*-xylene (97%), *p*-xylene (99.5%), methyl acetate (98%), phenylethyne and 1-bromohexane (98%) were purchased from Fluka (Steinheim, Germany).

Tetrapropylammonium chloride ($[N_{3333}^+][Cl^-]$, >97%) was purchased from Tokyo Chemical Industry (Portland, OR, USA). Trihexyl(tetradecyl)phosphonium chloride ($[P_{66614}^+][Cl^-]$, >93%) was purchased from Strem Chemical (Newburyport, MA, USA). Tetraethylammonium chloride ($[N_{2222}^+][Cl^-]$, >98%), tetrabutylammonium chloride ($[N_{4444}^+][Cl^-]$, >97%), $N_{4444}^+[Br^-]$ (>99%), allyl(triphenyl)phosphonium bromide ($[P_{Al(Ph)_3}][Br^-]$, 99%), tetrabutylphosphonium chloride ($[P_{4444}^+][Cl^-]$, 96%), hexanoic acid (Hex. A., >98%), octanoic acid (Oct. A., >99%), para-toluenesulfonic acid monohydrate (p-TSA, >98.5%), levulinic acid (Lev. A., 98%), benzene sulfonic acid (Benz. Sulf. A., 98%), benzaldehyde (99%), 5-bromoacenaphthene (90%), 2-nitronaphthalene (85%), 1-chlorohexane (99%), 1-chlorooctane (99%), cyclohexanol (99%), cyclohexanone (99.8%), 1-iodobutane (99%), iodoethane (99%) 1-nitropropane (98%), octylaldehyde (99%), 1-pentanol (99%), 2-pentanone (99%), propionitrile (99%), 1-decanol (99%), acetophenone (99%), aniline (99.5%), benzonitrile (99%), benzyl alcohol (99%), 1-bromooctane (99%), 2-butanol (98%), 1-butanol (99.8%), 1,2-dichlorobenzene (99%), dichloromethane (99.8%), 1,4-dioxane (99.5%), 1-octanol (99%), phenol (99%), pyridine (99%), pyrrole (98%), *m*-xylene (99.5%), 1-propanol (99.9%) 2-propanol (99.9%), methanol (99%), ethanol (99%), benzylamine (99%), benzamide (99%) and propionic acid (99%) were purchased from MilliporeSigma (St. Louis, MO, USA). Deuterated dimethyl sulfoxide (d_6 -DMSO) and deuterated chloroform ($CDCl_3$) were obtained from Cambridge Isotope Laboratories (Andover, MA, USA). The deactivated capillary used for coating DES was provided by MEGA (Legnano, MI, Italy).

Synthesis of DES

All the DES analyzed in this study have previously been reported literature.^{23,7,15,35,51} All DES were prepared by following a similar protocol as reported in literature. Firstly, equimolar amounts of the HBD and HBA were weighed in a 20 mL vial containing a magnetic stirrer. Then

the vial was heated for three hours at 60 °C, after which a uniform and homogenous mixture of DES was formed. These DES were placed in vacuum oven at room temperature for two days for drying. All DES were then characterized by ^{13}C and ^1H NMR.

Coating of DES as a stationary phase

All GC columns were coated with the DES using five-meter deactivated fused silica capillaries employing the static coating method. The coating solution was prepared by dissolving the DES in dichloromethane at a concentration of 0.45 % (w/v) to yield an approximate film thickness of 0.28 μm . The coated columns were conditioned at 70 °C for 30 min under a constant flow of helium. The column efficiency was determined using naphthalene at 70 °C with all columns possessing efficiencies above 2200 plates/meter.

For the inverse GC study, all probes were dissolved in dichloromethane at a concentration of 1 mg/mL. A list of the analytes used in this study are provided in Table S1 (table will be added in SI) and were injected isothermally at 40, 50, and 60 °C. Analytes exhibiting lower boiling points exhibited little to no retention on the stationary phase while other analytes retained strongly. For this reason, not all probe molecules were subjected to the solvation parameter model at some temperatures.

The GC measurements carried out on an Agilent 7890B gas chromatograph employing a flame ionization detector (GC-FID). Helium was used as a carrier gas at a flow rate of 1 mL/min. The injector and detector temperatures were held at 150 °C using a split ratio of 20:1 and an injection volume of 1 μL . Hydrogen was utilized as the makeup gas at a flow rate of 30 mL/min while the air flow was held at 400 mL/min for the FID. Propane was used to measure the dead volume of each column at 40, 50, and 60 °C. Multiple linear regression analysis and statistical calculations were conducted using the program Analyze-it (Microsoft, USA).

Results and Discussion

Solvation interactions of DES with various probe molecules were evaluated at temperatures of 40 °C, 50 °C, and 60 °C. A diverse and broad range of probe molecules were used to analyze these parameters to attain five different interaction parameters (see Table S1). The retention data of each probe on the DES were collected at three different temperatures to illustrate the change in the magnitude of solvation interactions with temperature. Two main classes of DES namely phosphonium and ammonium-based, were explored in this study. Tables 2 and 3 provide the interaction parameters (consisting of five different interactions), which were obtained from the retention times of the probe molecules chosen.

Amongst all of the ammonium-based DES, the hydrogen bond acidity (b) and the π - π / lone pair (e) interactions were found to be the weakest of all interaction and their magnitude was found to be close to zero indicating little or no interaction for all DES except $[\text{N}_{2222}^+][\text{Cl}^-]$: 2Lac. A. In comparison, the phosphonium-based DES also displayed similar behavior for the hydrogen bond acidity and the π - π / lone pair interactions for most of the DES except $[\text{P}_{\text{Al}(\text{Ph})_3}^+][\text{Br}^-]$: 3p-TSA, which is rich in aromatic moieties. The interaction parameter values for b and e for $[\text{N}_{2222}^+][\text{Cl}^-]$: 2Lac. A are 0.44 and 0.35, respectively at temperature of 50 °C. Similar trends for these interaction parameters have been seen upon the introduction of hydroxyl functional groups in the chemical structure in various ILs.⁵² The presence of hydroxyl groups in the HBD gives rise to n - π interactions and enhances the capability of the solvent to interact with basic probe molecules. Furthermore, aromatic moieties introduced in $[\text{P}_{\text{Al}(\text{Ph})_3}^+][\text{Br}^-]$: 3 p-TSA lead to an increase in π - π interactions between the solvent and probe molecules giving rise to a positive value of 0.27 for the π - π / lone pair interactions compared to $[\text{P}_{66614}^+][\text{Cl}^-]$ ($e = -0.16$) at 40 °C. A similar trend was observed for the e interaction parameter where ILs possessing multiple aryl groups within the

cation displayed high π - π with analytes such as polycyclic aromatic hydrocarbons and polychlorinated biphenyls.⁵³ Dipolar interactions (*s*-term) for both classes of compounds were found to be relatively high compared to ILs. The dipolarity term of ammonium-based DES ranged from 1.97 to 2.52, while that of the phosphonium-based DES was 1.86 to 2.56 at 50 °C. The extent of dipolar interactions dropped when the relative ratio of HBA: HBD was changed from 1:1 to 1:2 for both ammonium and phosphonium-based DES when octanoic acid was used as the HBD. Similarly, dipolar interactions also decreased when the anion was varied from chloride to bromide, as shown in Table 2.⁴⁶

Moreover, dispersive interactions were larger for $[P_{66614}^+][Cl^-]$ -based DES compared to $[N_{4444}^+][Cl^-]$ -based DES, where they both possess the chloride anion but contain different cations. It has been previously established that cations possessing longer alkyl chains are beneficial for the separation of homologs of a homologous series.²³ For example, $[P_{66614}^+][Cl^-] : 2Oct. A.$ displayed higher retention factors for haloalkanes as compared to $[N_{4444}^+][Cl^-] : 2Oct. A.$ The retention factors for bromobutane, bromohexane, and bromooctane were 2.27, 6.97, and 46.35 for $[P_{66614}^+][Cl^-] : 2Oct. A. DES$, while those for $[N_{4444}^+][Cl^-] : 2Oct. A.$ were 0.94, 5.42, and 32.19, respectively. Furthermore, when both HBA and HBD possessed shorter alkyl chain substituents, the magnitude of dispersive interaction is found to be significantly lower compared to those containing longer alkyl chains in HBA and HBD. The magnitude of the “*l*” value for $[N_{2222}^+][Cl^-] : 2Lac. A.$ and $[N_{2222}^+][Cl^-] : 2Lev. A.$ are 0.45 and 0.56, respectively. The extent of dispersive interactions is relatively greater for DES possessing Lev. A. as HBA as compared to DES containing Lac. A. as HBA, since Lev. A. has longer alkyl chain length. The DES $[P_{66614}^+][Cl^-] : 2Oct. A.$ displayed the highest dispersive interactions (0.81 at 50 °C) compared to the other solvents.

Effect of the hydrogen bond acceptor

Ammonium and phosphonium halide-based DES have been characterized in this study to further understand their role in the molecular interactions. The cation center, alkyl chain length, and halide anion have been altered to examine their effect on DES solvation interactions. The $[P_{66614}^+][Cl^-]$ as well as $[N_{4444}^+][Cl^-]$ ILs were characterized as benchmarks for comparison purposes. The values for the hydrogen bond basicity term (a) for $[P_{66614}^+][Cl^-]$ was lower (7.36) than that of $[N_{4444}^+][Cl^-]$ (8.03) at 50 °C, as shown in Tables 2 and 3. This is consistent with the previously reported interaction parameters for these salts.^{46,48} The hydrogen bond basicity values were found to be higher for ammonium-based DES as compared to analogous phosphonium-based DES.

The alkyl chain length of HBA was systematically modulated to study its contribution towards the solvation properties. The capability of DES to interact with acidic solutes was observed to significantly decrease when the alkyl chain length in cation of HBA is shorten from butyl to ethyl in the $[N_{4444}^+][Cl^-] : 2Oct. A.$, $[N_{3333}^+][Cl^-] : 2Oct. A.$ and $[N_{2222}^+][Cl^-] : 2Oct. A.$ This results in a decrease in the hydrogen bond basicity (a) value from 6.80, 5.43, and 5.02 at 50 °C, respectively. This decrease in hydrogen bonding interaction with acidic probe molecules can be attributed to stronger intramolecular electrostatic interactions among the cation and the anion of HBA.^{54,55}

The halogen anion within the HBA acts as a hydrogen bond acceptor by participating in hydrogen bonding with an acidic proton of the HBD. When the anion in the $[N_{4444}^+][X^-] : 2Oct. A$ DES (where X^- is the halide anion) is changed from $[Cl^-]$ to $[Br^-]$, the dipolarity/polarizability (s) and hydrogen bond basicity (a) interaction parameters were observed to be different as $[Cl^-]$ based DESs displayed higher values. The hydrogen bond basicity (a) term decreased from 7.60 for $[N_{4444}^+][Cl^-] : 2Oct. A.$ to 5.57 for $[N_{4444}^+][Br^-] : 2Oct. A.$ at 50 °C when the anion was changed

from chloride to bromide. Probes including 1-butanol, 1-pentanol, and cyclohexanol, exhibited stronger retention factors on the DES containing chloride as the anion compared to bromide as shown in Tables 2 and 4. Moreover, the dipolarity parameter decreased from 2.34 to 2.15 at 50 °C for $[N_{4444}^+][Cl^-] : 2Oct. A.$ and $[N_{4444}^+][Br^-] : 2Oct. A.$ respectively.

Effect of hydrogen bond donor

The extent of hydrogen bonding within the DES can be controlled by carefully modulating the type of HBD. Therefore, a diverse set of carboxylic acid-based HBDs with varying types of functional groups, varying pKa values, and varying chain lengths have been combined with ammonium and phosphonium-based HBAs. A summary of retention factors at 60 °C for alcohols and alkyl halides on the ammonium-based DES and neat $[N_{4444}^+][Cl^-]$ stationary phase is provided in Table 4. The data suggests that the hydrogen bonding occurring within the DES can be tailored by changing the pKa of acids (i.e. octanoic acid, benzenesulfonic acid, and malonic acid). The considerably high retention factors of mainly the alcohols on the neat $[N_{4444}^+][Cl^-]$ stationary phase shows the higher hydrogen bond basicity (*a*) term (7.70 at 60 °C). This is due to the free chloride ions being able to firmly hold the acidic protons as it is not being hindered.

As shown in Table 4, combining $[N_{4444}^+][Cl^-]$ with Oct. A. (pKa = 4.86) resulted in a decrease in the retention of acidic probes hence decreasing its hydrogen-bond basicity (*b* = 7.41) at 60 °C. The hydrogen bond basicity further reduced to 6.48 at 60 °C when two equivalents of Oct. A. were paired with $[N_{4444}^+][Cl^-]$. When stronger acids were possessing much lower pKa values were employed as HBDs such as, p-TSA (pKa = -2.8) and Benz. Sulf. A. (pKa = -6.7) was used as the donor; the hydrogen bond basicity decreased to 5.50 and 4.94 at 60 °C, respectively. The effect of functional groups capable of hydrogen bonding with the HBA was studied using malonic acid and lactic acid. Malonic acid is dioic acid (pKa₁ = 2.83) while lactic acid (pKa =

3.86) contains a carboxyl, and a hydroxyl functional group within its structure. When both acids were paired with $[N_{4444}^+][Cl^-]$ at 1 to 2 molar ratios, it was observed that the retention factors of acidic molecules drastically decreased compared DES composed of Oct. A. When the chain length of the HBD is varied from octanoic acid to hexanoic acid in $[N_{4444}^+][Cl^-] : 2\text{Oct. A.}$ and $[N_{4444}^+][Cl^-] : 2\text{Hex. A. DES}$, the hydrogen bond basicity (α) value decreased from 6.80 to 6.44, respectively.

Desulfurization of fuels with DES

Several different types of DES consisting of ammonium halide-based HBA and carboxylic acid-based HBD have shown potential towards the extractive desulfurization of fuels.¹⁷⁻¹⁹ Li et al. explored the extraction efficiencies of DES consisting of choline chloride, tetramethylammonium chloride, tetrabutylammonium chloride HBA combined with various mono, dicarboxylic acids and alcohol-based HBDs.¹⁷ The highest extraction efficiencies were found for DES containing $[N_{4444}^+][Cl^-]$ as its HBA along with a monocarboxylic acid such as octanoic acid and phenylacetic acid. The extraction efficiencies decreased by approximately 25% as the monocarboxylic acid (octanoic acid) was replaced by a dicarboxylic acid (malonic acid). This study concluded that the main driving force behind the desulfurization process is the hydrogen bonding interaction between the DES and the thiol functional group of the sulfur-containing moieties in the fuels.¹⁷ Table 2 shows that the hydrogen bond basicity DES decreases as the HBD is changed from two equivalents Oct. A. (6.80) to two equivalents Mal. A. (4.41) while containing the same HBA ($[N_{4444}^+][Cl^-]$). Similarly, the extraction efficiencies further decreased when the chain length within the cation of HBA was shorten from tetrabutyl to tetramethyl.¹⁷ A similar trend can be seen in DES possessing the same octanoic acid HBD with different HBAs where basicity values change significantly as $[N_{4444}^+][Cl^-]$ ($\alpha = 6.80$), $[N_{3333}^+][Cl^-]$ ($\alpha = 5.43$), and $[N_{2222}^+][Cl^-]$ ($\alpha = 5.02$) at 50 °C as the HBD, as shown in Table2 . As the alkyl chain length of HBA decreases or the number carboxyl or hydroxyl functional groups increases the capability of DES of hydrogen

bonding interaction towards molecules with like thiophene, benzothiophene and dibenzothiophenes also decreases.¹⁷

Extraction of natural products Cynaropicrin

DES containing the tetraalkylammonium halide-based HBA and carboxylic acid-based HBD have been used for extraction of Cynaropicrin, a bioactive compound of great potential for its application in nutraceutical applications.^{36,56} The extraction efficiency of $[N_{2222}^+][Cl^-]$ -based DES was found to be lower than that of tetrabutylammonium halide. For example, the reaction yield for Cynaropicrin (wt%) using $[N_{4444}^+][Cl^-] : 2$ Hex. A was determined 2.4% while $[N_{2222}^+][Cl^-] : 2$ Hex. A was found to be 0.4%.³⁶ This can be related to the lower hydrogen bonding capability of DES when the alkyl chain length is decreased. A similar set of DES in which the alkyl chain length substituent in the HBA cation is decreased from butyl to ethyl demonstrated a significant drop in the capability of DES to form hydrogen bonds with solute molecules. For example the hydrogen bond basicity value for $[N_{4444}^+][Cl^-] : 2$ Oct. A. was found to be 6.80 and decreased to 5.02 for $[N_{2222}^+][Cl^-] : 2$ Oct. A. at 50 °C, as shown in Table 2. This decreased alkyl chain length results in stronger intramolecular electrostatic interactions which decreases the extent of hydrogen bonding with Cynaropicrin, and results in lower extraction efficiencies. The higher basicity for chloride compared to bromide gives rise to a higher extent of hydrogen bonding, resulting in higher hydrogen bond basicity value in the experimental quantification of solvation interactions in this study. The extraction yields of Cynaropicrin (wt%) for $[N_{4444}^+][Cl^-] : 2$ Oct. A and $[N_{4444}^+][Br^-] : 2$ Oct. A were 2.7% and 1.7%, respectively. The hydroxyl groups in the Cynaropicrin were more selective towards chloride-based DES and this concurs with the findings of de Faria et. al.³⁶ The experimental data shows that the alcohols in this study retain significantly longer on the $[N_{4444}^+][Cl^-]$ ($a = 6.80$ at 50 °C) DES compared to the $[N_{4444}^+][Br^-]$ ($a = 5.57$ at 50 °C)

analogue. The extraction efficiencies were found to be the highest (2.84%) at a temperature of 25 °C followed by a drop to 2.47% at 35 °C, then further decreased to 2.29% at 45 °C.³⁶ This trend is fully supported by the interaction parameters determined in this study where an increase in temperature resulted in a decrease in interaction by hydrogen bonding. Therefore, it is not surprising to observe decrease in extraction efficiencies of analytes where hydrogen bonding is the major driving force towards extraction.

Conclusion

Twenty combinations of deep eutectic solvents containing ammonium and phosphonium as its HBAs and carboxylic acid groups as the HBD was designed for the characterization using a linear free energy relationship. Compared to the Kamlet-Taft parameters and normalized solvent polarity scales, the inverse GC approach was able to characterize DESs containing similar functionality with minor changes such as the molar ratio, pKa of acid, and chain length of both HBA and HBD. The chloride-based DESs displayed superior hydrogen basicity compared to the bromide analogs. The retention factors at 50 °C of butanol, cyclohexanol, and hexanol were 98.86, 484.90, and 553.40 for [N₄₄₄₄⁺][Cl⁻] : 2Oct. A, while on the [N₄₄₄₄⁺][Br⁻] : 2Oct. A column, the values were 28.67, 160.58, and 160.9, respectively. The pKa of the HBD played an important role in the overall basicity of the solvents as less acidic donors displayed higher interaction parameters for basicity while the reverse trend was observed with more acidic donors. The pure [P₆₆₆₁₄⁺][Cl⁻] ionic liquid displayed a hydrogen bond basicity (*a*) value of 7.72 at 40 °C while [P₆₆₆₁₄⁺][Cl⁻] : 2Oct. A (pKa = 4.89) had a basicity value of 7.20 at 40 °C. When *p*-toluenesulfonic acid (pKa = -6.5) and benzenesulfonic acid (pKa = -2.5) acted as donors for the same HBA, the basicity values decrease to 5.83 and 5.04, respectively. Understanding the solvation properties of DES can further improve the trial and error process when choosing these solvents for different applications.

References

- (1) Abbott, A. P.; Capper, G.; Davies, D. L.; Rasheed, R. K.; Tambyrajah, V. Novel Solvent Properties of Choline Chloride/Urea Mixtures. *Chem. Commun.* **2003**, 9 (1), 70–71.
- (2) Abbott, A. P.; Boothby, D.; Capper, G.; Davies, D. L.; Rasheed, R. K. Deep Eutectic Solvents Formed between Choline Chloride and Carboxylic Acids: Versatile Alternatives to Ionic Liquids. *J. Am. Chem. Soc.* **2004**, 126 (29), 9142–9147.
- (3) Smith, E. L.; Abbott, A. P.; Ryder, K. S. Deep Eutectic Solvents (DESs) and Their Applications. *Chem. Rev.* **2014**, 114 (21), 11060–11082.
- (4) Kollau, L. J. B. M.; Vis, M.; Van Den Bruinhorst, A.; Esteves, A. C. C.; Tuinier, R. Quantification of the Liquid Window of Deep Eutectic Solvents. *Chem. Commun.* **2018**, 54 (95), 13351–13354.
- (5) Florindo, C.; Branco, L. C.; Marrucho, I. M. Quest for Green-Solvent Design: From Hydrophilic to Hydrophobic (Deep) Eutectic Solvents. *ChemSusChem* **2019**, 12 (8), 1549–1559.
- (6) Paiva, A.; Craveiro, R.; Aroso, I.; Martins, M.; Reis, R. L.; Duarte, A. R. C. Natural Deep Eutectic Solvents - Solvents for the 21st Century. *ACS Sustain. Chem. Eng.* **2014**, 2 (5), 1063–1071.
- (7) Rodriguez Rodriguez, N.; MacHiels, L.; Binnemans, K. P-Toluenesulfonic Acid-Based Deep-Eutectic Solvents for Solubilizing Metal Oxides. *ACS Sustain. Chem. Eng.* **2019**, 7 (4), 3940–3948.
- (8) Xu, P.; Zheng, G. W.; Zong, M. H.; Li, N.; Lou, W. Y. Recent Progress on Deep Eutectic Solvents in Biocatalysis. *Bioresour. Bioprocess.* **2017**, 4 (1), 34.
- (9) Pätzold, M.; Siebenhaller, S.; Kara, S.; Liese, A.; Syldatk, C.; Holtmann, D. Deep Eutectic Solvents as Efficient Solvents in Biocatalysis. *Trends Biotechnol.* **2019**, 37 (9), 943–959.
- (10) Huang, Z. L.; Wu, B. P.; Wen, Q.; Yang, T. X.; Yang, Z. Deep Eutectic Solvents Can Be Viable Enzyme Activators and Stabilizers. *J. Chem. Technol. Biotechnol.* **2014**, 89 (12), 1975–1981.
- (11) Zubeir, L. F.; Van Osch, D. J. G. P.; Rocha, M. A. A.; Banat, F.; Kroon, M. C. Carbon Dioxide Solubilities in Decanoic Acid-Based Hydrophobic Deep Eutectic Solvents. *J. Chem. Eng. Data* **2018**, 63 (4), 913–919.
- (12) Haider, M. B.; Jha, D.; Kumar, R.; Marriyappan Sivagnanam, B. Ternary Hydrophobic Deep Eutectic Solvents for Carbon Dioxide Absorption. *Int. J. Greenh. Gas Control* **2020**, 92, 102839.

- (13) Dai, Y.; Witkamp, G.-J.; Verpoorte, R.; Choi, Y. H. Natural Deep Eutectic Solvents as a New Extraction Media for Phenolic Metabolites in *Carthamus Tinctorius* L. *Anal. Chem.* **2013**, *85* (13), 6272–6278.
- (14) Williamson, S. T.; Shahbaz, K.; Mjalli, F. S.; AlNashef, I. M.; Farid, M. M. Application of Deep Eutectic Solvents as Catalysts for the Esterification of Oleic Acid with Glycerol. *Renew. Energy* **2017**, *114*, 480–488.
- (15) Hayyan, A.; Ali Hashim, M.; Mjalli, F. S.; Hayyan, M.; AlNashef, I. M. A Novel Phosphonium-Based Deep Eutectic Catalyst for Biodiesel Production from Industrial Low Grade Crude Palm Oil. *Chem. Eng. Sci.* **2013**, *92*, 81–88.
- (16) Wang, X.; Jiang, W.; Zhu, W.; Li, H.; Yin, S.; Chang, Y.; Li, H. A Simple and Cost-Effective Extractive Desulfurization Process with Novel Deep Eutectic Solvents. *RSC Adv.* **2016**, *6* (36), 30345–30352.
- (17) Li, C.; Li, D.; Zou, S.; Li, Z.; Yin, J.; Wang, A.; Cui, Y.; Yao, Z.; Zhao, Q. Extraction Desulfurization Process of Fuels with Ammonium-Based Deep Eutectic Solvents. *Green Chem.* **2013**, *15* (10), 2793–2799.
- (18) Li, J. J.; Xiao, H.; Tang, X. D.; Zhou, M. Green Carboxylic Acid-Based Deep Eutectic Solvents as Solvents for Extractive Desulfurization. *Energy and Fuels* **2016**, *30* (7), 5411
- (19) Gutiérrez, A.; Atilhan, M.; Aparicio, S. Theoretical Study of Oil Desulfuration by Ammonium-Based Deep Eutectic Solvents. *Energy and Fuels* **2018**, *32* (7), 7497–7507.
- (20) Abbott, A. P.; Al-Barzinjy, A. A.; Abbott, P. D.; Frisch, G.; Harris, R. C.; Hartley, J.; Ryder, K. S. Speciation, Physical and Electrolytic Properties of Eutectic Mixtures Based on $\text{CrCl}_3 \cdot 6\text{H}_2\text{O}$ and Urea. *Phys. Chem. Chem. Phys.* **2014**, *16* (19), 9047–9055.
- (21) Abbott, A. P.; Capper, G.; Davies, D. L.; Rasheed, R. K. Ionic Liquid Analogues Formed from Hydrated Metal Salts. *Chem. - A Eur. J.* **2004**, *10* (15), 3769–3774.
- (22) Zhang, J.; Wu, T.; Chen, S.; Feng, P.; Bu, X. Versatile Structure-Directing Roles of Deep Eutectic Solvents and Their Implication in the Generation of Porosity and Open Metal Sites for Gas Storage. *Angew. Chemie Int. Ed.* **2009**, *48* (19), 3486–3490.
- (23) Teles, A. R. R.; Capela, E. V.; Carmo, R. S.; Coutinho, J. A. P.; Silvestre, A. J. D.; Freire, M. G. Solvatochromic Parameters of Deep Eutectic Solvents Formed by Ammonium-Based Salts and Carboxylic Acids. *Fluid Phase Equilib.* **2017**, *448*, 15–21.
- (24) Madeira, P. P.; Loureiro, J. A.; Freire, M. G.; Coutinho, J. A. P. Solvatochromism as a New Tool to Distinguish Structurally Similar Compounds. *J. Mol. Liq.* **2019**, *274*, 740–745.

- (25) Zhang, J.; Yu, L.; Gong, R.; Li, M.; Ren, H.; Duan, E. Role of Hydrophilic Ammonium-Based Deep Eutectic Solvents in SO₂ Absorption. *Energy and Fuels* **2019**.
- (26) Florindo, C.; Lima, F.; Ribeiro, B. D.; Marrucho, I. M. Deep Eutectic Solvents: Overcoming 21st Century Challenges. *Curr. Opin. in Green Sustain. Chem.* 2019, 31–36.
- (27) Radošević, K.; Cvjetko Bubalo, M.; Gaurina Srček, V.; Grgas, D.; Landeka Dragičević, T.; Redovniković, R. I. Evaluation of Toxicity and Biodegradability of Choline Chloride Based Deep Eutectic Solvents. *Ecotoxicol. Environ. Saf.* **2015**, 112, 46–53.
- (28) Zhao, B. Y.; Xu, P.; Yang, F. X.; Wu, H.; Zong, M. H.; Lou, W. Y. Biocompatible Deep Eutectic Solvents Based on Choline Chloride: Characterization and Application to the Extraction of Rutin from *Sophora Japonica*. *ACS Sustain. Chem. Eng.* **2015**, 3 (11), 2746–2755.
- (29) Juneidi, I.; Hayyan, M.; Hashim, M. A. Evaluation of Toxicity and Biodegradability for Cholinium-Based Deep Eutectic Solvents. *RSC Adv.* **2015**, 5 (102), 83636–83647.
- (30) Reichardt, C. Solvatochromic Dyes as Solvent Polarity Indicators. *Chem. Rev.* **1994**, 94 (8), 2319–2358.
- (31) Poole, C. F. Chromatographic and Spectroscopic Methods for the Determination of Solvent Properties of Room Temperature Ionic Liquids. *J. Chromatogr. A.* 28, **2004**, 49–82.
- (32) Kamlet, M. J.; Taft, R. W. The Solvatochromic Comparison Method. I. The .Beta.-Scale of Solvent Hydrogen-Bond Acceptor (HBA) Basicities. *J. Am. Chem. Soc.* **1976**, 98 (2), 377–383.
- (33) Yokoyama, T.; Taft, R. W.; Kamlet, M. J. The Solvatochromic Comparison Method. 3. Hydrogen Bonding by Some 2-Nitroaniline Derivatives. *J. Am. Chem. Soc.* **1976**, 98 (11), 3233–3237.
- (34) Poole, C. F. Chromatographic and Spectroscopic Methods for the Determination of Solvent Properties of Room Temperature Ionic Liquids. *J. Chromatogr. A* **2004**, 1037 (1–2), 49–82.
- (35) Florindo, C.; McIntosh, A. J. S.; Welton, T.; Branco, L. C.; Marrucho, I. M. A Closer Look into Deep Eutectic Solvents: Exploring Intermolecular Interactions Using Solvatochromic Probes. *Phys. Chem. Chem. Phys.* **2017**, 20 (1), 206–213.
- (36) de Faria, E. L. P.; do Carmo, R. S.; Cláudio, A. F. M.; Freire, C. S. R.; Freire, M. G.; Silvestre, A. J. D. Deep Eutectic Solvents as Efficient Media for the Extraction and Recovery of Cynaropicrin from *Cynara Cardunculus* L. Leaves. *Int. J. Mol. Sci.* **2017**, 18 (11), 1–8.
- (37) Pandey, A.; Rai, R.; Pal, M.; Pandey, S. How Polar Are Choline Chloride-Based Deep Eutectic Solvents? *Phys. Chem. Chem. Phys.* **2014**, 16 (4), 1559–1568.

- (38) Zhekenov, T.; Toksanbayev, N.; Kazakbayeva, Z.; Shah, D.; Mjalli, F. S. Formation of Type III Deep Eutectic Solvents and Effect of Water on Their Intermolecular Interactions. *Fluid Phase Equilib.* **2017**, *441*, 43–48.
- (39) Mokhtarpour, M.; Shekaari, H.; Zafarani-Moattar, M. T.; Golgoun, S. Solubility and Solvation Behavior of Some Drugs in Choline Based Deep Eutectic Solvents at Different Temperatures. *J. Mol. Liq.* **2020**, *297*, 111799.
- (40) Anderson, J. L.; Ding, J.; Welton, T.; Armstrong, D. W. Characterizing Ionic Liquids on the Basis of Multiple Solvation Interactions. *J. Am. Chem. Soc.* **2002**, *124* (47), 14247–14254.
- (41) Etxeberría, A.; Alfageme, J.; Uriarte, C.; Iruin, J. J. Inverse Gas Chromatography in the Characterization of Polymeric Materials. *J. Chromatogr. A* **1992**, *607* (2), 227–237.
- (42) Abraham, M. H. Scales of Solute Hydrogen-Bonding: Their Construction and Application to Physicochemical and Biochemical Processes. *Chemical Society Reviews.* **1993**, 73–83.
- (43) Abraham, M. H.; Andonian-Haftvan, J.; Whiting, G. S.; Leo, A.; Taft, R. S. Hydrogen Bonding. Part 34. The Factors That Influence the Solubility of Gases and Vapours in Water at 298 K, and a New Method for Its Determination. *J. Chem. Soc. Perkin Trans. 2* **1994**, 1777–1791.
- (44) Abraham, M. H. Characterization of Some GLC Chiral Stationary Phases: LFER Analysis. *Anal. Chem.* **1997**, *69* (4), 613–617.
- (45) Abraham, M. H.; Poole, C. F.; Poole, S. K. Classification of Stationary Phases and Other Materials by Gas Chromatography. *J. Chromatogr. A* **1999**, *842* (1–2), 79–114.
- (46) Poole, S. K.; Poole, C. F. Chemometric Evaluation of the Solvent Properties of Liquid Organic Salts. *Analyst* **1995**, *120* (2), 289–294.
- (47) Zhao, Q.; Eichhorn, J.; Pitner, W. R.; Anderson, J. L. Using the Solvation Parameter Model to Characterize Functionalized Ionic Liquids Containing the Tris(Pentafluoroethyl)Trifluorophosphate (FAP) Anion. *Anal. Bioanal. Chem.* **2009**, *395* (1), 225–234.
- (48) Armstrong, D. W.; Breitbach, Z. S. Characterization of Phosphonium Ionic Liquids through a Linear Solvation Energy Relationship and Their Use as GLC Stationary Phases. *Anal. Bioanal. Chem.* **2008**, *390* (6), 1605–1617.
- (49) Van Noort, P. C. M.; Haftka, J. J. H.; Parsons, J. R. Updated Abraham Solvation Parameters for Polychlorinated Biphenyls. *Environ. Sci. Technol.* **2010**, *44* (18), 7037–7042.

- (50) Körner, S.; Albert, J.; Held, C. Catalytic Low-Temperature Dehydration of Fructose to 5-Hydroxymethylfurfural Using Acidic Deep Eutectic Solvents and Polyoxometalate Catalysts. *Front. Chem.* **2019**, *7*, 1–11.
- (51) Phelps, T. E.; Bhawawet, N.; Jurisson, S. S.; Baker, G. A. Efficient and Selective Extraction of $^{99m}\text{TcO}_4^-$ from Aqueous Media Using Hydrophobic Deep Eutectic Solvents. *ACS Sustain. Chem. Eng.* **2018**, *6* (11), 13656–13661.
- (52) Huang, K.; Han, X.; Zhang, X.; Armstrong, D. W. PEG-Linked Geminal Dicationic Ionic Liquids as Selective, High-Stability Gas Chromatographic Stationary Phases. *Anal. Bioanal. Chem.* **2007**, *389* (7), 2265–2275.
- (53) Odugbesi, G. A.; Nan, H.; Soltani, M.; Davis, J. H.; Anderson, J. L. Ultra-High Thermal Stability Perarylated Ionic Liquids as Gas Chromatographic Stationary Phases for the Selective Separation of Polyaromatic Hydrocarbons and Polychlorinated Biphenyls. *J. Chromatogr. A* **2019**, 460-466.
- (54) Boyd, R. H. Lattice Energies and Hydration Thermodynamics of Tetra-Alkylammonium Halides. *J. Chem. Phys.* **1969**, *51* (4), 1470–1474.
- (55) Fernandes, A. M.; Rocha, M. A. A.; Freire, M. G.; Marrucho, I. M.; Coutinho, J. A. P.; Santos, L. M. N. B. F. Evaluation of Cation-Anion Interaction Strength in Ionic Liquids. *J. Phys. Chem. B* **2011**, *115* (14), 4033–4041.
- (56) Elsebai, M. F.; Mocan, A.; Atanasov, A. G. Cynaropicrin: A Comprehensive Research Review and Therapeutic Potential as an Anti-Hepatitis C Virus Agent. *Frontiers in Pharmacol.* **2016**, 472.
- (57) Jiang, N.; Huang, R.; Qi, W.; Su, R.; He, Z. Effect of Formic Acid on Conversion of Fructose to 5-Hydroxymethylfurfural in Aqueous/Butanol Media. *Bioenergy Res.* **2012**, *5* (2), 380–386.
- (58) Tao, F.; Song, H.; Chou, L. Dehydration of Fructose into 5-Hydroxymethylfurfural in Acidic Ionic Liquids. *RSC Adv.* **2011**, *1* (4), 672–676.

Figures

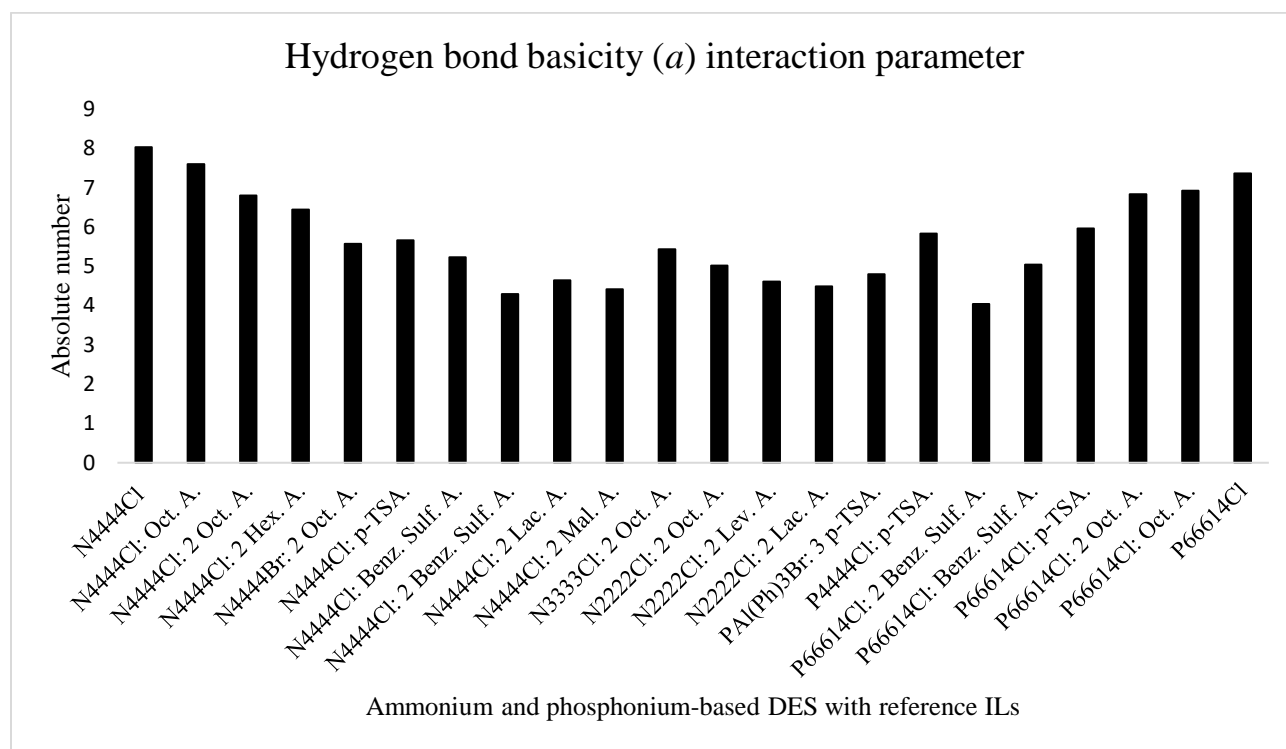


Figure 1. The magnitude of hydrogen bond basicity (*a*) at 50 °C for all the ammonium and phosphonium-based DES along with reference ILs

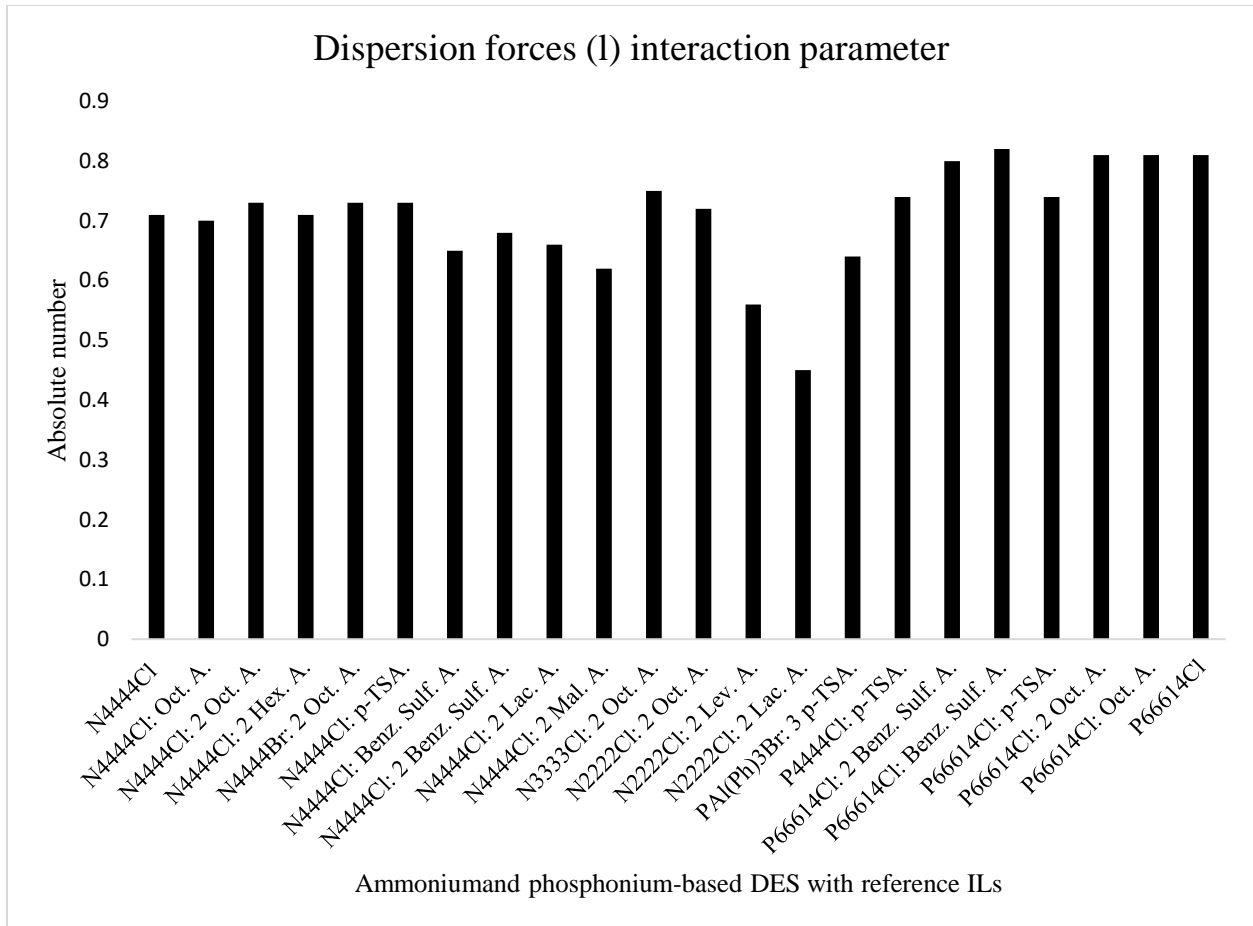


Figure 2. The magnitude of dispersion forces (l) at 50 °C for all the ammonium and phosphonium-based DES along with reference ILs

Tables

Table 1. Structure and composition twenty ammonium and phosphonium DES with different carboxylic acid groups as its donor

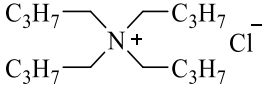
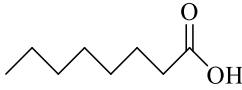
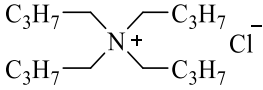

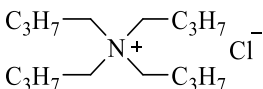
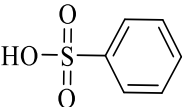
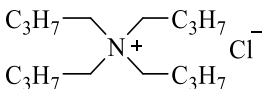
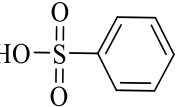
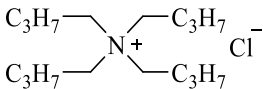
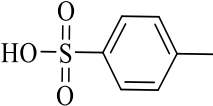
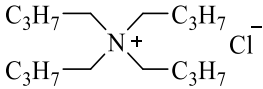
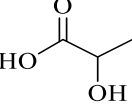
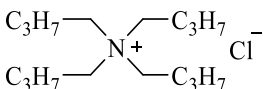
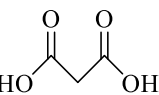
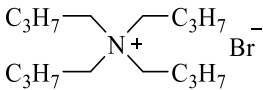
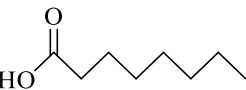
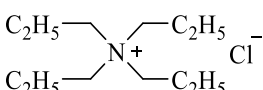
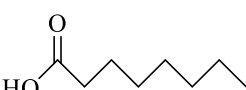
Sr #	HBA	HBD	Abbreviation of DES
Ammonium-based DES			
1			[N ₄₄₄₄ ⁺][Cl ⁻] : Oct. A.
2		2 	[N ₄₄₄₄ ⁺][Cl ⁻] : 2Oct. A.
3			[N ₄₄₄₄ ⁺][Cl ⁻] : Benz. Sulf. A.
4		2 	[N ₄₄₄₄ ⁺][Cl ⁻] : 2Benz. Sulf. A.
5			[N ₄₄₄₄ ⁺][Cl ⁻] : p-TSA.
6		2 	[N ₄₄₄₄ ⁺][Cl ⁻] : 2Lac. A.
7		2 	[N ₄₄₄₄ ⁺][Cl ⁻] : 2Mal. A.
8		2 	[N ₄₄₄₄ ⁺][Br ⁻] : 2Oct. A.
9		2 	[N ₃₃₃₃ ⁺][Cl ⁻] : 2Oct. A.

Table 1 continued

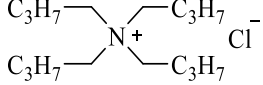
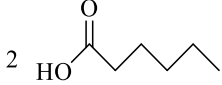
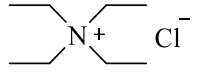
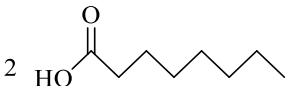
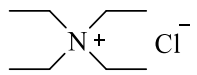
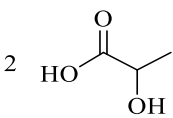
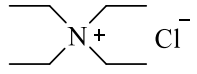
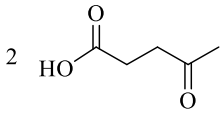
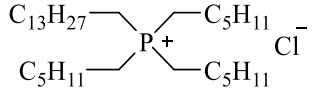
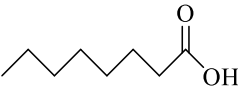
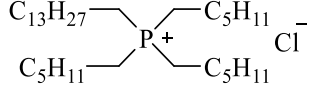

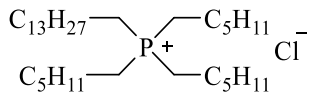
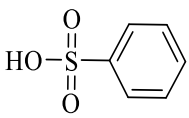
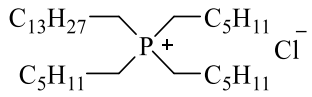
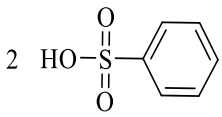
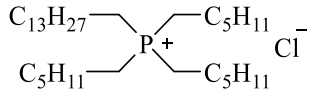
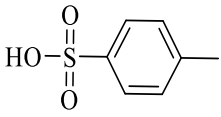
Sr #	HBA	HBD	Abbreviation of DES
Ammonium-based DES			
10		2 	[N ₄₄₄₄ ⁺][Cl ⁻] : 2Hex. A.
11		2 	[N ₂₂₂₂ ⁺][Cl ⁻] : 2Oct. A.
12		2 	[N ₂₂₂₂ ⁺][Cl ⁻] : 2Lac. A.
13		2 	[N ₂₂₂₂ ⁺][Cl ⁻] : 2Lev. A.
Phosphonium-based DES			
14			[P ₆₆₆₁₄ ⁺][Cl ⁻] : Oct. A.
15		2 	[P ₆₆₆₁₄ ⁺][Cl ⁻] : 2Oct. A.
16			[P ₆₆₆₁₄ ⁺][Cl ⁻] : Benz. Sulf. A.
17		2 	[P ₆₆₆₁₄ ⁺][Cl ⁻] : 2Benz. Sulf. A.
18			[P ₆₆₆₁₄ ⁺][Cl ⁻] : p-TSA.

Table 1 continued

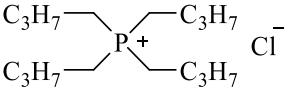
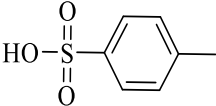
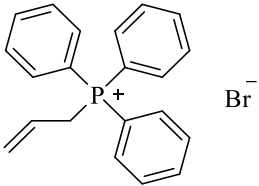
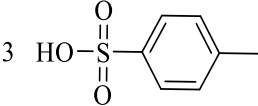
Sr #	HBA	HBD	Abbreviation of DES
Phosphonium-based DES			
19			[P ₆₆₆₁₄ ⁺][Cl ⁻] : p-TSA.
20		3 	[P _{Al(Ph)₃} ⁺][Cl ⁻] : 3p-TSA.

Table 2. Interaction parameters for ten ammonium-based DES obtained from the Solvation Parameter model. The ionic liquid [N₄₄₄₄⁺][Cl⁻] was included for comparison

DES	Temperature (°C)	Interaction parameters						<i>n</i> ^a	<i>R</i> ^{2 a}	<i>F</i> ^a
		<i>c</i>	<i>e</i>	<i>s</i>	<i>a</i>	<i>b</i>	<i>l</i>			
[N ₄₄₄₄ ⁺][Cl ⁻] : Oct. A.	40	-3.38 (0.10)	0 (0)	2.67 (0.11)	8.11 (0.16)	-0.43 (0.14)	0.76 (0.02)	39	0.99	774
	50	-3.31 (0.09)	0 (0)	2.52 (0.11)	7.60 (0.16)	-0.40 (0.14)	0.70 (0.02)	39	0.99	803
	60	-3.35 (0.09)	0 (0)	2.50 (0.11)	7.41 (0.16)	-0.53 (0.13)	0.68 (0.02)	39	0.99	776
[N ₄₄₄₄ ⁺][Cl ⁻] : 2Oct. A.	40	-3.16 (0.08)	-0.18 (0.08)	2.41 (0.10)	7.13 (0.15)	-0.36 (0.13)	0.77 (0.02)	39	0.99	884
	50	-3.18 (0.07)	-0.16 (0.07)	2.34 (0.10)	6.80 (0.14)	-0.38 (0.12)	0.73 (0.02)	39	0.99	960
	60	-3.19 (0.07)	-0.14 (0.06)	2.26 (0.09)	6.48 (0.13)	-0.38 (0.11)	0.69 (0.02)	39	0.99	1037
[N ₄₄₄₄ ⁺][Cl ⁻] : 2Hex. A.	40	-3.17 (0.09)	0 (0)	2.36 (0.11)	7.00 (0.17)	-0.32 (0.14)	0.75 (0.02)	38	0.99	739
	50	-3.14 (0.08)	0 (0)	2.25 (0.10)	6.44 (0.15)	-0.32 (0.12)	0.71 (0.02)	38	0.99	840
	60	-3.11 (0.07)	-0.14 (0.07)	2.17 (0.09)	5.92 (0.13)	-0.36 (0.11)	0.67 (0.02)	38	0.99	849
[N ₄₄₄₄ ⁺][Cl ⁻] : Benz. Sulf. A.	40	-3.07 (0.07)	-0.20 (0.07)	2.48 (0.08)	5.34 (0.12)	-0.38 (0.11)	0.72 (0.02)	41	0.99	1015
	50	-3.12 (0.06)	-0.20 (0.06)	2.46 (0.08)	5.23 (0.11)	-0.44 (0.10)	0.68 (0.01)	41	0.99	1134
	60	-3.19 (0.06)	-0.17 (0.06)	2.38 (0.08)	4.94 (0.11)	-0.38 (0.10)	0.66 (0.01)	41	0.99	1029

Table 2 continued

DES	Temperature (°C)	Interaction parameters						n^a	R^{2a}	F^a
		c	e	s	a	b	l			
[N ₄₄₄₄ ⁺][Br ⁻] : 2Oct. A.	40	-3.18 (0.07)	-0.21 (0.07)	2.24 (0.09)	5.88 (0.13)	-0.46 (0.11)	0.79 (0.02)	36	0.99	1026
	50	-3.13 (0.07)	-0.17 (0.07)	2.15 (0.09)	5.57 (0.13)	-0.42 (0.11)	0.73 (0.02)	35	0.99	914
	60	-3.13 (0.05)	-0.19 (0.05)	2.05 (0.06)	5.05 (0.09)	-0.43 (0.08)	0.71 (0.01)	36	0.99	1621
[N ₄₄₄₄ ⁺][Cl ⁻] : 2 Benz. Sulf. A.	40	-3.23 (0.06)	-0.14 (0.06)	2.52 (0.08)	4.54 (0.13)	0 (0)	0.70 (0.01)	40	0.99	1111
	50	-3.19 (0.06)	0 (0)	2.40 (0.07)	4.29 (0.11)	0 (0)	0.65 (0.01)	40	0.99	1225
	60	-3.22 (0.05)	0 (0)	2.31 (0.06)	4.00 (0.10)	0 (0)	0.62 (0.01)	40	0.99	1337
[N ₄₄₄₄ ⁺][Cl ⁻] : p-TSA	40	-3.20 (0.07)	-0.32 (0.07)	2.58 (0.09)	5.99 (0.14)	-0.59 (0.12)	0.78 (0.02)	38	0.99	969
	50	-3.20 (0.07)	-0.28 (0.07)	2.49 (0.09)	5.66 (0.13)	-0.58 (0.11)	0.73 (0.02)	38	0.99	988
	60	-3.16 (0.07)	-0.24 (0.07)	2.42 (0.09)	5.50 (0.13)	-0.60 (0.11)	0.69 (0.02)	38	0.99	892
[N ₄₄₄₄ ⁺][Cl ⁻] : 2Mal. A.	40	-3.09 (0.06)	0 (0)	2.31 (0.07)	4.78 (0.11)	0 (0)	0.66 (0.01)	39	0.99	1302
	50	-3.11 (0.05)	0 (0)	2.24 (0.06)	4.41 (0.10)	0 (0)	0.62 (0.01)	38	0.99	1330
	60	-3.15 (0.05)	0 (0)	2.17 (0.06)	4.04 (0.10)	0 (0)	0.58 (0.01)	39	0.99	1422
[N ₄₄₄₄ ⁺][Cl ⁻] : 2Lac. A.	40	-2.93 (0.07)	0 (0)	2.20 (0.09)	5.03 (0.14)	0 (0)	0.68 (0.02)	38	0.99	832
	50	-3.06 (0.05)	0 (0)	2.16 (0.06)	4.64 (0.10)	0 (0)	0.66 (0.01)	38	0.99	1351
	60	-3.02 (0.05)	0 (0)	2.08 (0.06)	4.25 (0.09)	0 (0)	0.61 (0.01)	38	0.99	1467
[N ₃₃₃₃ ⁺][Cl ⁻] : 2Oct. A.	40	-3.04 (0.08)	0 (0)	2.15 (0.10)	5.96 (0.16)	-0.47 (0.13)	0.77 (0.02)	37	0.99	705
	50	-3.06 (0.07)	0 (0)	2.05 (0.09)	5.43 (0.14)	-0.45 (0.11)	0.75 (0.01)	37	0.99	822
	60	-2.99 (0.07)	-0.22 (0.07)	1.91 (0.09)	5.09 (0.14)	-0.55 (0.12)	0.73 (0.01)	37	0.99	658

Table 2 continued

DES	Temperature (°C)	Interaction parameters						n^a	R^2^a	F^a
		c	e	s	a	b	l			
[N ₂₂₂₂ ⁺][Cl ⁻] : 2Oct. A.	40	-3.13 (0.06)	0 (0)	2.04 (0.08)	5.30 (0.12)	-0.29 (0.10)	0.78 (0.02)	38	0.99	1155
	50	-3.22 (0.06)	0 (0)	1.97 (0.07)	5.02 (0.11)	-0.23 (0.09)	0.72 (0.01)	37	0.99	1204
	60	-3.07 (0.05)	0 (0)	1.93 (0.07)	4.86 (0.10)	-0.26 (0.09)	0.66 (0.01)	38	0.99	1306
[N ₂₂₂₂ ⁺][Cl ⁻] : 2Lac. A.	40	-3.12 (0.05)	0.45 (0.05)	2.41 (0.06)	4.73 (0.10)	0.37 (0.08)	0.48 (0.01)	38	0.99	1601
	50	-3.14 (0.05)	0.44 (0.05)	2.35 (0.06)	4.49 (0.09)	0.35 (0.08)	0.45 (0.01)	38	0.99	1709
	60	-3.18 (0.04)	0.43 (0.05)	2.29 (0.06)	4.25 (0.09)	0.36 (0.07)	0.42 (0.01)	38	0.99	1730
[N ₂₂₂₂ ⁺][Cl ⁻] : 2Lev. A.	40	-3.30 (0.08)	0 (0)	2.44 (0.10)	4.80 (0.16)	0 (0)	0.59 (0.02)	38	0.99	604
	50	-3.38 (0.09)	0 (0)	2.40 (0.11)	4.61 (0.17)	0 (0)	0.56 (0.02)	38	0.99	476
	60	-3.34 (0.07)	0.16 (0.07)	2.28 (0.09)	4.36 (0.14)	0 (0)	0.52 (0.02)	38	0.99	644
[N ₄₄₄₄ ⁺][Cl ⁻]	40 ^b	-2.33 (0.10)	0.22 (0.10)	1.14 (0.14)	4.81 (0.19)	0 (0)	0.66 (0.03)	26	0.99	372
	50	-3.24 (0.12)	0 (0)	2.72 (0.15)	8.03 (0.22)	-0.53 (0.14)	0.71 (0.03)	35	0.99	501
	60	-3.24 (0.10)	0 (0)	2.60 (0.13)	7.70 (0.19)	-0.44 (0.12)	0.67 (0.02)	39	0.99	609

^a n , number of probe analytes subjected to multiple linear regression; R^2 , correlation coefficient; F , Fisher coefficients. ^b At 40 °C the thin layer of compound turns solid

Table 3. Interaction parameters for seven phosphonium-based DESs obtained from the solvation parameter model. The ionic liquid $[P_{66614}^+][Cl^-]$ was included for comparison

DES	Temperature (°C)	Interaction parameters								
		<i>c</i>	<i>e</i>	<i>s</i>	<i>a</i>	<i>b</i>	<i>l</i>	<i>n</i> ^a	<i>R</i> ^{2 a}	<i>F</i> ^a
$[P_{66614}^+][Cl^-]$: Oct. A.	40	-3.10 (0.08)	-0.28 (0.08)	2.09 (0.10)	7.20 (0.15)	-0.56 (0.13)	0.85 (0.02)	39	0.99	952
	50	-3.19 (0.08)	-0.22 (0.07)	1.98 (0.09)	6.92 (0.14)	-0.44 (0.12)	0.81 (0.02)	38	0.99	924
	60	-3.12 (0.08)	0 (0)	1.79 (0.10)	6.51 (0.15)	-0.45 (0.12)	0.76 (0.02)	38	0.99	847
$[P_{66614}^+][Cl^-]$: 2Oct. A.	40	-3.05 (0.10)	-0.23 (0.09)	2.00 (0.12)	6.98 (0.18)	-0.57 (0.14)	0.82 (0.02)	37	0.99	571
	50	-3.16 (0.08)	-0.20 (0.07)	1.92 (0.10)	6.83 (0.15)	-0.50 (0.11)	0.81 (0.02)	37	0.99	825
	60	-3.12 (0.08)	-0.18 (0.07)	1.83 (0.09)	6.45 (0.14)	-0.42 (0.11)	0.77 (0.02)	37	0.99	812
$[P_{66614}^+][Cl^-]$: Benz. Sulf. A.	40	-2.98 (0.07)	-0.46 (0.07)	2.04 (0.08)	5.34 (0.12)	-0.68 (0.10)	0.86 (0.02)	41	0.99	1077
	50	-2.98 (0.06)	-0.43 (0.06)	1.97 (0.08)	5.04 (0.11)	-0.67 (0.10)	0.82 (0.02)	41	0.99	1181
	60	-2.97 (0.06)	-0.34 (0.06)	1.82 (0.07)	4.72 (0.10)	-0.59 (0.09)	0.77 (0.01)	41	0.99	1147
$[P_{66614}^+][Cl^-]$: 2 Benz. Sulf. A.	40	-3.01 (0.06)	-0.40 (0.06)	2.03 (0.08)	4.28 (0.13)	-0.39 (0.11)	0.83 (0.02)	39	0.99	917
	50	-3.07 (0.07)	-0.35 (0.06)	1.91 (0.08)	4.04 (0.12)	-0.39 (0.10)	0.80 (0.01)	40	0.99	1068
	60	-2.95 (0.05)	-0.26 (0.05)	1.72 (0.07)	3.56 (0.10)	0.30 (0.09)	0.74 (0.01)	39	0.99	1112
$[P_{66614}^+][Cl^-]$: p-TSA.	40	-3.23 (0.07)	-0.32 (0.07)	2.62 (0.09)	6.20 (0.15)	-0.58 (0.12)	0.77 (0.02)	37	0.99	1004
	50	-3.27 (0.07)	-0.30 (0.07)	2.56 (0.09)	5.96 (0.14)	-0.62 (0.12)	0.74 (0.02)	37	0.99	972
	60	-3.26 (0.06)	-0.33 (0.06)	2.51 (0.08)	5.63 (0.13)	-0.60 (0.11)	0.69 (0.01)	37	0.99	1015

Table 3 continued

DES	Temperature (°C)	Interaction parameters								
		<i>c</i>	<i>e</i>	<i>s</i>	<i>a</i>	<i>b</i>	<i>l</i>	<i>n</i> ^a	<i>R</i> ^{2 a}	<i>F</i> ^a
[P ₄₄₄₄ ⁺][Cl ⁻] : p-TSA.	40	-3.18 (0.07)	-0.35 (0.07)	2.58 (0.10)	6.06 (0.14)	-0.56 (0.12)	0.78 (0.02)	37	0.99	915
	50	-3.25 (0.07)	-0.32 (0.07)	2.52 (0.10)	5.83 (0.14)	-0.57 (0.12)	0.74 (0.02)	37	0.99	855
	60	-3.17 (0.07)	-0.30 (0.07)	2.41 (0.09)	5.48 (0.13)	-0.60 (0.11)	0.69 (0.02)	37	0.99	864
[P _{AlPh₃} ⁺][Br ⁻] : 3 p-TSA.	40	-3.29 (0.06)	0.27 (0.06)	1.91 (0.08)	5.12 (0.12)	0.70 (0.10)	0.67 (0.01)	36	0.99	1144
	50	-3.29 (0.06)	0.27 (0.06)	1.86 (0.07)	4.80 (0.11)	0.63 (0.09)	0.64 (0.01)	36	0.99	1160
	60	-3.32 (0.06)	0.28 (0.06)	1.82 (0.07)	4.49 (0.11)	0.59 (0.09)	0.60 (0.01)	36	0.99	1086
[P ₆₆₆₁₄ ⁺][Cl ⁻]	40	-2.92 (0.09)	0 (0)	2.11 (0.11)	7.72 (0.17)	-0.69 (0.14)	0.80 (0.02)	37	0.99	814
	50	-3.07 (0.09)	-0.26 (0.08)	2.06 (0.10)	7.36 (0.15)	-0.59 (0.13)	0.81 (0.02)	39	0.99	845
	60	-3.12 (0.07)	-0.22 (0.07)	1.99 (0.10)	6.94 (0.14)	-0.54 (0.12)	0.77 (0.02)	40	0.99	970

^a *n*, number of probe analytes subjected to multiple linear regression; *R*², correlation coefficient; *F*, Fisher coefficients.

Table 4. Retention factors of ten alcohols on ammonium-based DES with varying hydrogen bond donors at 60 °C. The molten salt N₄₄₄₄Cl was included for comparison.

Probe	N ₄₄₄₄ Cl	N ₄₄₄₄ Cl : 2Oct. A.	N ₄₄₄₄ Cl : p-TSA.	N ₄₄₄₄ Cl : 2Benz. Sulf. A.	N ₄₄₄₄ Cl : 2Lac. A.	N ₄₄₄₄ Cl : 2Mal. A.
1-butanol	163.63	53.85	19.62	5.43	9.76	6.77
1-pentanol	361.01	117.50	39.89	12.11	20.56	13.65
1-hexanol	765.49	269.32	86.26	26.22	42.62	27.31
cyclopentanol	375.52	120.29	45.03	15.39	23.74	16.91
cyclohexanol	747.27	246.46	89.23	33.36	48.82	35.27
2-propanol	26.38	2.21	3.24	2.18	1.90	1.40
methanol	26.04	8.18	3.99	0.88	1.83	1.10
ethanol	30.22	9.85	4.76	1.26	2.21	1.68
2-butanol	71.49	18.11	6.46	2.14	3.64	2.48
1-propanol	52.39	23.44	7.64	2.51	4.56	3.25
1-chlorobutane	0.51	0.43	0.40	0.24	0.30	0.21
1-chlorohexane	2.27	2.07	1.85	0.98	1.23	0.82
1-bromohexane	2.35	2.13	3.86	1.98	2.42	1.67
1-bromooctane	10.45	10.53	16.87	7.94	9.56	6.19
naphthalene	182.92	128.29	118.31	94.18	99.55	83.54
nitrobenzene	304.38	157.99	163.42	102.80	101.76	84.78

Supplemental

Table S1 List of all probe molecules and their corresponding solute descriptors used to characterize IL-based stationary phases employing the solvation parameter model

Probe molecule	E	S	A	B	L
Acetic acid	0.265	0.65	0.61	0.44	1.75
Acetophenone	0.818	1.01	0	0.48	4.501
Aniline	0.955	0.96	0.26	0.41	3.934
Benzaldehyde	0.82	1	0	0.39	4.008
Benzene	0.61	0.52	0	0.14	2.786
Benzonitrile	0.742	1.11	0	0.33	4.039
Benzyl alcohol	0.803	0.87	0.33	0.56	4.221
Bromoethane	0.366	0.4	0	0.12	2.62
1-Bromooctane	0.339	0.4	0	0.12	5.09
1-Butanol	0.224	0.42	0.37	0.48	2.601
Butyraldehyde	0.187	0.65	0	0.45	2.27
2-Chloroaniline	1.033	0.92	0.25	0.31	4.674
1-Chlorobutane	0.21	0.4	0	0.1	2.722
1-Chlorohexane	0.201	0.4	0	0.1	3.777
1-Chlorooctane	0.191	0.4	0	0.1	4.772
<i>p</i> -Cresol	0.82	0.87	0.57	0.31	4.312
Cyclohexanol	0.46	0.54	0.32	0.57	3.758
Cyclohexanone	0.403	0.86	0	0.56	3.792
1,2-Dichlorobenzene	0.872	0.78	0	0.04	4.518
<i>N,N</i> -Dimethylformamide	0.367	1.31	0	0.74	3.173
1,4-Dioxane	0.329	0.75	0	0.64	2.892
Ethyl acetate	0.106	0.62	0	0.45	2.314
Ethyl benzene	0.613	0.51	0	0.15	3.778
1-Iodobutane	0.628	0.4	0	0.15	4.13
Methyl caproate	0.067	0.6	0	0.45	3.844
Naphthalene	1.34	0.92	0	0.2	5.161
Nitrobenzene	0.871	1.11	0	0.28	4.557
1-Nitropropane	0.242	0.95	0	0.31	2.894
1-Octanol	0.199	0.42	0.37	0.48	4.619
Octylaldehyde	0.16	0.65	0	0.45	4.361
1-Pentanol	0.219	0.42	0.37	0.48	3.106
2-Pentanone	0.143	0.68	0	0.51	2.755
Ethyl phenyl ether	0.681	0.7	0	0.32	4.242
Phenol	0.805	0.89	0.6	0.3	3.766
Propionitrile	0.162	0.9	0.02	0.36	2.082
Pyridine	0.631	0.84	0	0.52	3.022
Pyrrole	0.613	0.73	0.41	0.29	2.865
Toluene	0.601	0.52	0	0.14	3.325
<i>m</i> -Xylene	0.623	0.52	0	0.16	3.839

Table S1continued

Probe molecule	E	S	A	B	L
<i>o</i> -Xylene	0.663	0.56	0	0.16	3.939
<i>p</i> -Xylene	0.613	0.52	0	0.16	3.839
2-Propanol	0.212	0.36	0.33	0.56	1.764
2-Nitrophenol	1.015	1.05	0.05	0.37	4.76
1-Bromohexane	0.349	0.4	0	0.12	4.13
Propionic acid	0.233	0.65	0.6	0.45	2.29
1-Decanol	0.191	0.42	0.37	0.48	5.628
Methanol	0.278	0.44	0.43	0.47	0.97
Ethanol	0.246	0.42	0.37	0.48	1.485
Nitromethane	0.313	0.95	0.06	0.31	1.892
Cyclopentanol	0.427	0.54	0.32	0.56	3.241
Cycloheptanol	0.513	0.54	0.32	0.58	4.407
Phenylethyne	0.679	0.58	0.12	0.24	3.692
1-Hexanol	0.21	0.42	0.37	0.48	3.61
Bromobutane	0.36	0.4	0	0.12	3.105
Iodoethane	0.64	0.4	0	0.15	2.573
Methylacetate	0.142	0.64	0	0.45	1.911
2-Butanol	0.217	0.36	0.33	0.56	2.338
1-Propanol	0.236	0.42	0.37	0.48	2.031

CHAPTER 4. GENERAL CONCLUSION

This thesis describes the use of ionic liquids and deep eutectic solvents as new materials for GC stationary phases for the separation of analytes. Both ILs and DESs are room temperature liquids possessing negligible vapor pressure making them great candidates for stationary phases.

Chapter 2 describes the use of six highly thermally stable ILs containing aryl substituents for the separation of polycyclic aromatic hydrocarbons and polychlorinated biphenyls. Compared to commercial PDMS-based stationary phases, these high-temperature ILs displayed similar retention behavior while providing selectivity at high oven temperatures. At temperatures between the ranges of 300-350 °C, baseline separation for isomer pairs anthracene and phenanthrene was obtained on five IL-based stationary phases out of the six in the study. Five-meter segments of each column were subjected to stepwise heating experiments to evaluate the stability of the stationary phase. Column efficiencies were measured after each heating experiment to gain insight into the degradation/volatilization of the stationary phase. ILs 4 and 5 displayed superior thermal stability up to 350 °C while the remaining ILs were stable in the temperature range of 290-310 °C.

Chapter 3 discusses the incorporation of deep eutectic solvents as gas chromatographic stationary phases to better understand their solvation properties. While DES have been characterized via spectroscopic methods, there are some limitations as to the sensitivity of the solvatochromic probes used. In this chapter of the thesis, various interaction parameters of the stationary phase including, non-bonding or π - π interactions, dipolarity/polarizability, hydrogen bond basicity, hydrogen bond acidity, and the dispersion forces were studied. Twenty DESs composed of ammonium and phosphonium HBAs with varying carboxylic acid HBDs were synthesized to characterize their different interaction

parameters. All DES-based stationary phases possessed similar hydrogen bond acidity and nonbonding capabilities. The data in this study suggests that the ability of the free chloride anion to interact can be modulated by choice of HBA and HBD. More acidic donors appear to decrease the hydrogen bond basicity of the stationary phase, where DESs containing less acidic donors showed the opposite trend. Future work aims to explore the use of choline chloride, which is commonly used as the HBA, to develop a database for selecting DESs for targeted applications.